Prepandemic personal concentrations of per- and polyfluoroalkyl substances (PFAS) and other pollutants: Specific and combined effects on the incidence of COVID-19 disease and SARS-CoV-2 infection

José Pumarega[a,b,c,*], Magda Gasull[b,c,d], Jani Koponen[e], Laura Campi[b], Panu Rantakokko[e], Luis A. Henríquez-Hernández[f,g], Ruth Aguilar[h], Carolina Donat-Vargas,[c,i,j] Manuel Zumbado[f,g], Judit Villar-García[b], Cristina Rius[c,d,k], Pablo Santiago-Díaz[b], Marta Vidal[h,l], Alfons Jimenez[h,l], Mar Iglesias[b], Carlota Dobaño[h,l,¶], Gemma Moncunill[h,l,¶], Miquel Porta[a,b,c,d*]

[a] *School of Medicine, Universitat Autònoma de Barcelona, Barcelona, Spain*

[b] *Hospital del Mar Research Institute, Barcelona, Spain*

[c] *CIBER de Epidemiología y Salud Pública (CIBERESP), Barcelona, Spain*

[d] *Universitat Pompeu Fabra, Barcelona, Spain*

[e] *Finnish Institute for Health and Welfare (THL), Kuopio, Finland*

[f] *Toxicology Unit, Research Institute of Biomedical and Health Sciences (IUIBS), Universidad de Las Palmas de Gran Canaria, Canary Islands, Spain*

[g] *CIBER de Obesidad y Nutrición (CIBEROBN), Madrid, Spain*

[h] *ISGlobal, Hospital Clínic - Universitat de Barcelona, Barcelona, Spain*

[i] *ISGlobal, Campus Mar, Barcelona, Spain*

[j] *Cardiovascular and Nutritonal Epidemiology Unit, Institut of Enviornmental Medicine, Karolinska Institutet, Stockholm, Sweden.*

[k] *Agència de Salut Pública de Barcelona, Barcelona, Spain*

[l] *CIBER de Enfermedades Infecciosas (CIBERINFEC), Barcelona, Spain*

* Corresponding authors at: Hospital del Mar Research Institute, Carrer del Dr. Aiguader 88, E-08003 Barcelona, Catalonia, Spain.

ORCID ID: http://orcid.org/0000-0003-1684-7428.

E-mail address: jpumarega@imim.es and mporta@imim.es (J. Pumarega and M. Porta).

[¶]These authors contributed equally.

H I G H L I G H T S

- With a clear time sequence, this is the only prospective cohort study on the topic.
- We analyzed 120 chemicals, including the 8 PFAS most usually detected.
- Such PFAS were not associated with SARS-CoV-2 seropositivity or COVID-19.
- Adjusting for PFAS, mixtures of POPs and elements remained associated with COVID-19.
- Some POPs and elements contribute to explain the heterogeneity in the two outcomes.

Running title: PFAS, COVID-19 and SARS-CoV-2.

Abbreviations: BHS, Barcelona Health Survey; BMI, body mass index; CI, confidence interval; COVID-19, coronavirus disease 2019; DDD, p,p'-dichlorodiphenyldichloroethane (p,p'-isomer); DDE, dichlorodiphenyldichloroethene (p,p'-isomer); DDT, p,p'-dichlorodiphenyltrichloroethane (p,p'-isomer); HCB, hexachlorobenzene; HCH, hexachlorocyclohexane; LOD, limit of detection; LOQ, limit of quantification; OCPs, organochlorine pesticides; OR, odds ratio; PAHs, polycyclic aromatic hydrocarbons; PBDEs, polybrominated diphenyl ethers; PCBs, polychlorinated biphenyls; PFAS, per- and polyfluoroalkyl substances; PFOA, perfluorooctanoic acid; PFDA, perfluorodecanoic acid; PFHxS, perfluorohexane sulfonate; PFNA perfluorononanoic acid; PFOS, perfluorooctane sulfonate; PFUnDA, perfluoroundecanoic acid; POPs, persistent organic pollutants; SARS-CoV-2, severe acute respiratory syndrome coronavirus 2.

Keywords:
per- and polyfluoroalkyl substances (PFAS)
SARS-CoV-2
COVID-19
Mixtures
Immunotoxicity

Funding

The work was supported in part by research grants from Instituto de Salud Carlos III, Government of Spain, co-funded by FEDER (FIS PI17/00088, FIS PI21/00052, and CIBER de Epidemiología y Salud Pública - CIBERESP); CRUE-Santander Fondo Supera Covid-19 (15072020); the Hospital del Mar Medical Research Institute (IMIM), Barcelona; and the Government of Catalonia (2017 SGR 439; 2021 SGR 43). GM is supported by RYC2020-029886-I/AEI/10.13039/501100011033, co-funded by European Social Fund (ESF). Development of SARS-CoV-2 reagents was partially supported by the NIAID Centers of Excellence for Influenza Research and Surveillance (CEIRS) contract HHSN272201400008C. ISGlobal acknowledges support from the Spanish Ministry of Science and Innovation and State Research Agency through the 'Centro de Excelencia Severo Ochoa 2019-2023' Program (CEX2018-000806-S), and support from the Generalitat de Catalunya through the CERCA Program. The funders had no role in study design, data collection and analysis, decision to publish, or preparation of the manuscript.

A B S T R A C T

Objective: To investigate the specific and combined effects of personal concentrations of some per- and polyfluoroalkyl substances (PFAS), other persistent organic pollutants (POPs), and chemical elements –measured in individuals' blood several years before the pandemic– on the development of SARS-CoV-2 infection and COVID-19 disease in the general population.

Methods: We conducted a prospective cohort study in 240 individuals from the general population of Barcelona. PFAS, other POPs, and chemical elements were measured in plasma, serum, and whole blood samples, respectively, collected in 2016-2017. PFAS were analyzed by liquid chromatography-triple quadrupole mass spectrometry. SARS-CoV-2 infection was detected by rRT-PCR in nasopharyngeal swabs and/or antibody serology in blood samples collected in 2020-2021.

Results: No individual PFAS nor their mixtures were significantly associated with SARS-CoV-2 seropositivity or COVID-19 disease. Previously identified mixtures of POPs and elements (Porta et al., 2023) remained significantly associated with seropositivity and COVID-19 when adjusted for PFAS (all OR > 4 or $p<0.05$). Nine chemicals comprised mixtures associated with COVID-19: thallium, ruthenium, lead, benzo[b]fluoranthene, DDD, other DDT-related compounds, manganese, tantalum, and aluminium. And nine chemicals comprised the mixtures more consistently associated with SARS-CoV-2 seropositivity: thallium, ruthenium, lead, benzo[b]fluoranthene, DDD, gold, and (protectively) selenium, indium, and iron.

Conclusions: The PFAS studied were not associated with SARS-CoV-2 seropositivity or COVID-19. The results confirm the associations between personal blood concentrations of some POPs and chemical elements and the risk of COVID-19 and SARS-CoV-2 infection in what remains the only prospective and population-based cohort study on the topic. Mixtures of POPs and chemical elements may contribute to explain the heterogeneity in the risks of SARS-CoV-2 infection and COVID-19 in the general population.

1. Introduction

Perfluoroalkyl and polyfluoroalkyl substances (PFAS) comprise several thousand chemicals whose common properties include high repellency to both water and oil, as well as thermal and chemical stability. They are used in a wide variety of industrial processes and consumer products, including waterproof coats, swimming apparel, stain resistant textiles, cooling, heavy industries, electronics, energy technologies, medical and dental products, food container linings, insecticide formulations, floor waxes, or surfactants. Human exposure to PFAS occurs mainly through drinking water, food, food packaging and other food-contact materials (including cookware), textiles, house dust, cosmetics, cleaning agents, electronic devices, and many other goods.[1-6]

Atmospheric and aqueous releases during manufacturing, use, and disposal have resulted in PFAS planetary contamination, and some analyses suggest that we have exceeded the safe operating space of the planetary boundary of contamination by PFAS. Because of the high persistence (which may act as a multiplier of toxicity), poor reversibility, and low social visibility of environmental exposure to PFAS and their associated effects, systemic and global policies to rapidly restrict PFAS uses and emissions are of vital importance for human and environmental health.[7-11]

The systemic ubiquity, persistence and bioaccumulation of PFAS explain their wide and –since their introduction in the 1940s– increasing presence in humans, documented for more than 50 years. The effects on human health have been studied to some extent for only a few PFAS, suggesting that they may be risk factors for pathological alterations in immune and inflammatory responses, endocrine and reproductive functions, metabolism, lipid patterns, obesity, liver enzymes, cardiovascular factors, and some cancers.[1-5,12]

Concerns about how PFAS exposure may affect the risk of COVID-19 are scientifically sound. Exposure to PFAS (usually, but not always, at high levels) may impact the immune system. A review of the U.S. National Toxicology Program found that exposure to perfluorooctanoic acid (PFOA) and perfluorooctane sulfonate (PFOS) is an immune hazard to humans, based on a high level of evidence that PFOA and PFOS suppressed the antibody response from animals, and a moderate level of evidence from studies in humans. Research is ongoing to understand how human contamination from PFAS may affect the risk of developing COVID-19.[13-15]

PFAS may decrease the effectiveness of some vaccines,[16-18] and the available evidence on this issue may have implications for research on the influence of PFAS and other environmental pollutants on the effectiveness of COVID-19 vaccines.[19-21] However, such issues are only partly related to the putative etiologic role of PFAS in COVID-19 (e.g., when COVID-19 vaccines were or are not available, or in other public health and clinical scenarios): PFAS may have a different influence on vaccine response and on the risk of COVID-19 disease. The present report will focus on the latter.

Surprisingly little is known about the effects of personal concentrations of environmental pollutants on the individual risk and the population incidence of COVID-19 disease.[22-27] This is partly due to the fact that –with one exception, so far[22]– no researchers have used blood samples collected before the pandemic to measure body concentrations of biomarkers of exposure to immunotoxic contaminants in individuals from the general population: such time sequence between exposure and effect is obviously required to analyze if the contaminants influenced the risk of SARS-CoV-2 infection and COVID-19. While praiseworthy, the only few studies that measured individual concentrations of contaminants or nutrients were based on individuals highly exposed to PFAS, whose blood samples were collected while already into the pandemic (aiming to assess vaccine response, not COVID-19 incidence),[19] on vaccinated healthcare workers with symptoms of COVID-19,[27] or on convenience samples from undefined groups of persons already infected or admitted to hospital with COVID-19.[23-26] Associations between drinking water contaminated by PFAS and the incidence of and mortality from COVID-19 were also observed in ecologic (aggregate) studies in two regions of Sweden and Italy; it was hypothesized that the associations might be explained by PFAS immunosuppression, bioaccumulation in lung tissue, or pre-existing diseases caused by PFAS.[28,29]

In what so far –to our knowledge– remains the only prospective and population-based study on the topic,[22] we observed strong associations between personal concentrations of some POPs and chemical elements (measured in serum and whole blood samples collected and archived 4 years before the pandemic) and the individual risk of SARS-CoV-2 infection and COVID-19. The results suggested that certain body concentrations of several mixtures of POPs and elements may contribute to explain the heterogeneity in the risk of SARS-CoV-2 infection and in the development of COVID-19 in the general population. However, the estimates of the associations[22] might be confounded by other unmeasured environmental contaminants, such as PFAS. Hence, we recently determined concentrations of PFAS in samples of plasma collected and archived at the same time as the blood samples in which we had measured concentrations of POPs and elements.

In other words, the rationale for the analyses summarized in the present report stems from two facts. First, there is wide, largely unexplained heterogeneity in immunological and clinical responses to SARS-CoV-2 infection.[30-33] Personal characteristics, comorbidities, lifestyles, living conditions, and the shared environment only partly account for such variation.[34-37] And second, PFAS, other POPs, and other environmental chemicals are immunoactive, and might affect the risk of COVID-19 through several systems.[5,30,34,36,38-44]

Therefore, the present study aimed to investigate the specific and combined effects of personal concentrations of some PFAS, other POPs, and chemical elements –measured in individuals' blood several years before the pandemic– on the development of SARS-CoV-2 infection and COVID-19 in the general population.

2. Methods

2.1. Study population

The present prospective cohort study was based on the Barcelona Health Survey (BHS) of 2016, whose methods have been described in detail.[22,45] The BHS generated a sample representative of the general, adult, non-institutionalized population of the city of Barcelona (Spain).[22,45-47] Through face-to-face interviews, the survey collected information about sociodemographic factors, chronic disorders, life styles, uses of healthcare services and preventive practices. At the end of the 2016 BHS interview, participants were offered to take part in a study on POPs and other contaminants, and 240 individuals accepted. Subsequently, a nurse interviewed again face-to-face such individuals, measured body parameters, and collected blood and urine samples.[22,45]

In all instances when biological samples were to be collected, participants had been asked to fast for at least eight hours before blood extraction. Blood was collected in two EDTA tubes, and in a vacuum system tube. One EDTA tube and the vacuum system tube were centrifuged for 15 minutes x 3000 rpm at 4ºC to obtain plasma and serum, respectively, and the second EDTA tube was used to collect and aliquot whole blood. Plasma, serum, and whole blood samples were stored at –80ºC.[22,45]

In October 2020, the 240 participants began to be invited to a follow-up visit, which 174 (72.5%) attended between 18 November 2020 and 7 June 2021.[22] During the follow-up visit a nurse measured their weight, height. It also collected new blood and urine samples, which constitute a crucial scientific resource of the present cohort study to analyze immunological and environmental components of the SARS-CoV-2 infection. The median time between the extraction of biological samples in 2016-2017 and 2020-2021 was 4.1 years. Compared to the 66 subjects who did not attend the follow-up visit, the 174 participants were more commonly women, younger, born in Catalonia, with a lower body mass index (BMI), more affluent, and with better self-perceived health.[22] The main analyses reported in the present paper are based on 154 of the 174 individuals who had not received any COVID-19 vaccine at the time of the follow-up visit.[22]

The Ethics Committee of the Parc de Salut Mar reviewed and approved the study protocols, and all participants signed an informed consent before sample collection and completing questionnaires.[45]

2.2. Socioeconomic and living conditions

Shortly before the follow-up visit in 2020-2021, the participants completed an online survey concerning signs and symptoms of COVID-19, diagnostic tests performed and their results, use of healthcare services, and vaccination, all during the previous months of the pandemic. This information was ascertained as well with the data base of the System of Diseases of Mandatory Reporting of the Agency of Public Health of Barcelona. The survey also elicited information on participants' lifestyle and living conditions during the pandemic.[22] During the visit, the nurse clarified answers to the online survey and asked further questions on vaccination, weight changes, and pregnancies. A household outdoor index was computed taking into account the number of individuals living in the same household, the availability and use of an outdoor space; the score of the index increased as the number of individuals increased and the availability and frequency of use of the outdoor space decreased. Other factors included in the online survey were: work conditions, use of public and private transport, and individual measures taken to avoid infection.[22]

2.3. Determination of SARS-CoV-2 infection and COVID-19 disease

2.3.1. SARS-CoV-2 infection

SARS-CoV-2 infection was determined at the Centre for Genomic Regulation (CRG) in all 174 members of the cohort who attended the follow-up visit in 2020-2021 by real time reverse-transcriptase polymerase chain reaction (rRT-PCR) in nasopharyngeal swabs. Briefly, samples were collected in 600 μL of lysis solution (DNA/RNA Shield, Zymo) to inactivate the virus, break membranes and stabilize the RNA. Samples were processed in a TECAN Dreamprep robot to isolate the RNA using the Quick-DNA/RNA Viral MagBead kit (Zymo; #R2140), and the purified RNA was analyzed by rRT-PCR in a ABI 7900 HT (384 wells) following the CDC standard procedure. Positive and negative controls were included in each assay plate. Among the 174 participants, there were 4 rRT-PCR-positives.[22]

To detect previous infections, SARS-CoV-2 antibody serological status of each participant was assessed in serum samples analyzed at the ISGlobal Immunology Laboratory in Barcelona. The levels [median fluorescence intensity (MFI)] of IgG, IgM and IgA were assessed by high-throughput multiplex quantitative suspension array technology, including 5 SARS-CoV-2 antigens.[22] Assay performance was previously established as 100% specificity and 95.78% sensitivity for seropositivity 14 days after symptoms onset.[30,48] Antigen-coupled microspheres were added to a 384-well μClear® flat bottom plate (Greiner Bio-One, Frickenhausen, Germany) in multiplex (2000 microspheres per analyte per well) in a volume of 90 μL of Luminex Buffer (1% BSA, 0.05% Tween 20, 0.05% sodium azide in PBS) using 384 channels Integra Viaflo semi-automatic device (96/384, 384 channel pipette). Hyperimmune pools were used as positive controls prepared at twofold, 8 serial dilutions from 1:12.5. Pre-pandemic samples were used as negative controls to estimate the cut-off of seropositivity. Ten microliter of each dilution of the positive control, negative controls and test samples (prediluted 1:50 in 96 round-bottom well plates), were added to the 384-well plate using Assist Plus Integra device with 12 channels Voyager pipette (final test sample dilution of 1:500). To quantify IgM and IgA, test samples and controls were pre-treated with anti-Human IgG (Gullsorb) at 1:10 dilution, to avoid IgG interferences. Technical blanks consisting of Luminex Buffer and microspheres without samples were added in 4 wells to control for non-specific signals. Assay positivity cut-offs specific for each isotype and analyte were calculated as 10 to the mean plus 3 standard deviations of $\log_{10}$-transformed MFI of the 240 pre-pandemic control samples collected in 2016-17. Results were defined as indeterminate when the MFI levels for a given isotype-analyte were between the positivity threshold and an upper limit at 10 to the mean plus 4.5 standard deviations of the $\log_{10}$-transformed MFIs of pre-pandemic samples, and no other isotype-antigen combination was above the positivity cut-off.[22,30]

Of the 154 participants mentioned above, 41 were SARS-CoV-2 seropositive (26.6%) (including all 4 positives by the follow-up rRT-PCR), 9 indeterminate (5.8%), and 104 seronegative (67.5%). There were no major differences in the main characteristics of seropositive and seronegative participants.[22]

2.3.2. COVID-19 disease

Cases of COVID-19 disease have been described in detail.[22] In total there were 20 cases of COVID-19 disease; all were seropositive for SARS-CoV-2 in our immunological assay, and all reported COVID-19 related symptoms. Specifically, 10 cases provided information of a positive diagnostic test for

SARS-CoV-2 infection (including all 4 positives at the follow-up rRT-PCR), and 2 or more COVID-19 related signs or symptoms; 2 were diagnosed of COVID-19 by a physician; and 8 had COVID-19 related signs or symptoms.[22,49] There were no major differences in the main characteristics of participants with and without COVID-19.[22]

2.4. Analytical chemical methods for PFAS

PFAS concentrations were measured in plasma samples at the National Institute for Health and Welfare in Finland, using a method based on liquid chromatography-triple quadrupole mass spectrometry (LC-MS/MS), described in detail elsewhere.[50] Plasma samples collected in 2016-2017 were stored until 2022 when concentrations of perfluorooctanoic acid (PFOA), perfluorodecanoic acid (PFDA), perfluorononanoic acid (PFNA), perfluoroundecanoic acid (PFUnDA), perfluorohexane sulfonate (PFHxS), and the linear and branched isomers forms of the perfluorooctane sulfonate (PFOS) were analyzed. These are currently the PFAS detected in 10% to 100% of participants in studies in the general population.[51-55]

The limit of quantification (LOQ) was 0.018 ng/mL for all individual PFAS. Quantifiable concentrations were detected for all the PFAS analyzed (range 45% for PFDA to 100% for linear PFOS) (Supplemental Table 1). When the concentration of a PFAS was below the LOQ, it was assigned the mid-value of this limit. The total PFOS was the sum of concentrations of both isomers (linear and branched); when the branched form of PFOS was below the LOQ, the value of the PFOS total was the value of the linear PFOS (Supplemental Tables 1 and 2). We detected and quantified a median of 6 PFAS per person (of a total of 7 PFAS, excluding PFOS total). Percentages of quantification and concentrations of PFAS in 2016 were similar in the 174 subjects who attended the follow-up visit in 2020 and in the 66 who did not (Supplemental Table 2).

2.5. Analytical chemical methods for POPs and elements

Analytical chemical methods for POPs and inorganic elements have also been described in detail.[22,44,45,50-59] Concentrations of 62 POPs and 50 chemical elements were analyzed in the Research Institute of Biomedical and Health Sciences (IUIBS) of the University of Las Palmas de Gran Canaria, Spain, in serum and whole blood samples (collected in 2016-2017), respectively.[22]

2.5.1. Analyses of POPs

Serum concentrations of the following POPs were measured: 38 organochlorine compounds (OCs) (20 organochlorine pesticides (OCPs), including six DDT-related compounds (*o,p'*-DDT, *p,p'*-DDT, *o,p'*-DDE, *p,p'*-DDE, *o,p'*-DDD, *p,p'*-DDD), and 18 polychlorinated biphenyls (PCBs)); 8 polybrominated diphenyl ethers (PBDEs); and 16 polycyclic aromatic hydrocarbons (PAHs).[22,45,56,57] The details of validated chromatographic methods and quality controls have been previously reported.[56,57,60] Half-milliliter aliquots of serum samples were mixed with 0.4 mL of water/n-propanol (85:15) and subsequently centrifuged at 3000 rpm for 5 minutes. Then, 0.1 mL of acetic acid was added to each sample and loaded to 200 mg (3 mL) Chromabond® C18ec columns (Macherey-Nagel, Germany) mounted in a vacuum manifold (Waters Corporation, USA). The analytes were eluted with 1 ml of dichloromethane. Briefly, we employed a Gas Chromatography (GC) System 7890B equipped with a 7693 Autosampler (Agilent Technologies, Palo Alto, CA, USA) for gas chromatographic separations.

The detection of the analytes was performed using a Triple Quad 7010 mass spectrometer (Agilent Technologies, Palo Alto, CA, USA). The quantification was done using point calibration curves, which were constructed using a least-squares linear regression from the injection of standard solutions ranging from 0.025 to 25 ng/mL.[45]

All measurements were performed in triplicate, and the geometric mean was used for the calculations. In each batch of samples, three controls were included for every 18 vials: a reagent blank consisting of a vial containing only cyclohexane; a vial containing 2 ng/mL of each of the pollutants in cyclohexane; and an internal laboratory quality control sample consisting of melted butter spiked at 10 ng/mL of each of the analytes, which was processed using the same method of extraction as the serum samples. The results were considered to be acceptable when the concentration of the analytes determined in the quality control sample was within 15% of the deviation of the theoretical value. Further details on quality of analyses and quality control were previously provided.[45,60]

Concentrations of total cholesterol and triglycerides were determined enzymatically, using serum obtained at the same time as the serum used for POP analyses. Total serum lipids were calculated by the standard formula 2 of Phillips et al.[22,45,46] POP concentrations were individually corrected for total lipids and are expressed in nanograms of analyte per gram lipid (ng/g of lipid).

2.5.2. Analyses of inorganic elements

The 50 inorganic elements analyzed included 9 essential inorganic elements, 15 elements from ATSDR's Substance Priority List of 2019,[43] 20 rare earth elements (REE), and 6 other minority elements commonly used in the manufacture of high-tech devices.[58,59]

100 mg of whole blood was weighed into quartz digestion tubes and then digested into 1 mL of acid solution (65% HNO_3) using a Milestone Ethos Up equipment (Milestone, Bologna, Italy). After cooling, the digested samples were transferred and diluted. An aliquot of each sample was taken and the internal standard was added for the analysis. The internal standard solution included scandium, germanium, rhodium and iridium (20 mg/mL each). Elements of standard purity (5% HNO_3, 100 mg/L) were purchased from CPA Chem (Stara Zagora, Bulgaria). Finally, two standard curves (range = 0.005–20 ng/mL) were made.[58]

2.6. Statistical analyses

Univariate statistics were computed as customary.[61] Spearman's rank correlation coefficient (ρ) was used to evaluate correlations between pairs of PFAS, other POPs, and elements (Supplemental Table 3). Among PFAS, high and statistically significantly correlations were observed between concentrations of PFDA, PFNA, PFUnDA and PFOS total and PFOS linear (all ρ's >0.7). ρ's >0.3 were observed among PFAS and PCBs, lead, arsenic, mercury, and selenium (Supplemental Figures 1 and 2). PFAS were weakly correlated with age, sex, household index, and BMI; they were not correlated with smoking or education.

Plasma concentrations of PFAS were initially categorized as quartiles. Cut-off points for quartiles were based on the distribution of the concentrations in the 240 participants (Supplemental Table 1).[22,45] Some PFAS were also dichotomized if no linear dose-response was apparent in quartile analyses, as

often documented in the literature, or if cell size was small.[22,42,44] PFAS concentrations were also analyzed as log-transformed continuous variables through linear regression models???.

Because a recent report suggested that the copper/selenium ratio (Cu/Se) may act as a biomarker of severity and immune response in SARS-CoV-2-infected patients,[27] we computed and analyzed such ratio in the 240 participants.

To assess the effect of the sum of multiple substances we computed for each participant *a)* the arithmetic sum of the concentrations of each substance in the set of substances of interest; and *b)* the sum of orders or sum of category rankings of the substances in the set of substances of interest by categorizing the concentrations of each compound in two or four categories, as appropriate, and adding for each participant the category number of each substance.[22]

The main effects of PFAS were independently explored in base models including the contaminant and potential confounders (data drawn from the online survey, personal interview, and follow-up visit).[22,61] To assess the effects of mixtures of POPs and other chemical elements, mutually adjusted, we selected models including from 2 to 5 contaminants that had been significant in base models, and we selected mixtures in which all substances showed significant associations with the outcome when including each one of the PFAS, in their log-transformed continuous form. To assess the magnitude of the associations, odds ratios (OR) between contaminants and outcomes (COVID-19 and SARS-CoV-2 seropositivity), with their corresponding 95% confidence intervals (CI) were computed through unconditional logistic regression.[61] ORs were adjusted for age, sex, tobacco smoking, BMI, education, the household outdoor index or other socioeconomic variables if such potentially confounding variables fulfilled pre-established criteria: $p \leq 0.5$ to enter the model and $p \leq 0.25$ to remain in it. To assess significance, we considered the magnitude of the association (e.g., OR > 4), the precision of the effect estimate, and the statistical significance ($p<0.05$).[22,61,62] We also used weighted quantile sum (WQS) regression to estimate a joint exposure effect of mixtures of PFAS on the risk of the outcomes, and no such mixtures were associated with any of the outcomes; such lack of association of mixtures of PFAS was also seen with logistic regression.[22,63] The level of statistical significance was set at 0.05 and all tests were two-tailed. Statistical analyses were conducted using R, version 4.2.1 (Boston, MA, 2021) (using version 3.0.4 of package gWQS), and SPSS version 22.0.0.0 (IBM SPSS Statistics, Armonk, NY, 2013).

3. Results

3.1. Associations with COVID-19 disease

No individual PFAS was statistically significantly associated with COVID-19 disease, and there were no monotonic patterns by quartiles (Table 1). When dichotomizing, PFDA was weakly positively related with COVID-19 disease (OR=2.32), whereas PFHxS and PFOS branched were weakly inversely associated with the disease (ORs=0.43, and OR=0.66, respectively) (all p>0.05) (Table 1). The sum of concentrations of the 5 PFAS (PFOA, PFDA, PFNA, PFUnDA and PFHxS) was also not associated with COVID-19, and combinations of PFAS, in pairs or other mixtures, were not associated with the disease either.

PFAS were not confounding our previous estimates of the effect of POPs and elements on the incidence of COVID-19 disease.[22] For instance, when such estimates were adjusted for PFOS branched or PFHxS, there were no changes or only slight changes in the ORs; e.g., we saw minor increases in the ORs for benzo[b]fluoranthene, thallium, aluminium, tantalum, and for the sums of PCBs 138-153-180 (Supplemental Table 4). Also compared with previous estimates,[22] a few POPs and elements had slightly reduced ORs, and all remained significant when adjusted for PFOS branched or for PFHxS. Therefore, several individual POPs and chemical elements continued to be associated with COVID-19 (ORs > 4 or p-values < 0.05). Other immunoactive substances and elements historically prevalent in humans remained unrelated[22] with the disease when adjusting for PFOS branched (Supplemental Table 4) or for PFHxS or other PFAS.

Previously identified[22] mixtures of POPs and elements also remained significantly associated with COVID-19 disease when adjusted for PFOS branched, while the latter was not associated with COVID-19 in any model (Table 2). Thus, mixtures of DDD, manganese, ruthenium, and tantalum (Table 2, model 1a); manganese, ruthenium, and tantalum (model 1b); DDD, ruthenium, and lead (model 2a); or DDE, manganese, benzo[b]fluoranthene, and tantalum (model 3b) had all substances (again, mutually adjusted, and adjusted for PFOS branched and confounders) significantly associated with the disease (all OR > 4 or p<0.05).

The median Cu/Se ratio was 0.38 (range: 0.18 to 0.90). Compared to participants with a ratio below the median, participants with a Cu/Se ratio above the median had a non-significant 40% decreased risk of developing COVID-19 disease (OR = 0.60, 95% CI: 0.22–1.67, p value = 0.329), adjusting for age, education, and smoking. The OR was very similar when PFOS branched was included in the model (OR = 0.52, 0.18–1.48, p = 0.216).

Remarkably, some mixtures included five substances, each independently associated with COVID-19. This was the case of DDT, ruthenium, lead, thallium, and benzo[b]fluoranthene (Table 2, model 4b, and

Figure 1), or of ruthenium, lead, thallium, manganese, and benzo[b]fluoranthene (model 5b). When part of a trio or a quartet comprising substances mentioned in Table 2, the OR for aluminium ranged from 8 to 18 (all $p < 0.05$ and, again, adjusted for PFOS branched and confounders) (e.g., models 7b, 8 and 9). With their different degrees of overlapping, models in Table 2 show the nine exposures that comprised the mixtures more consistently associated with COVID-19: thallium, ruthenium, lead, benzo[b]fluoranthene, DDD, other DDT-related compounds, manganese, tantalum, and aluminium.

3.2. Associations with SARS-CoV-2 seropositivity

No individual PFAS was significantly associated with SARS-CoV-2 seropositivity except PFHxS (only when dichotomized), and there were no monotonic patterns by quartiles (Table 3). No mixtures of two or more PFAS were associated with seropositivity.

PFAS were not confounding our previous estimates of the effect of POPs and elements on SARS-CoV-2 seropositivity.[22] When adjusting such estimates by PFHxS, most remained similar or slightly increased (Supplemental Table 5). Thus, the following individual POPs and elements continued to have ORs > 4 or $p < 0.05$: DDD, benzo(b)fluoranthene, lead, thallium, manganese, iron, gold, ruthenium, and the sum of orders of lead, thallium, manganese, tantalum, ruthenium, and benzo(b)fluoranthene.

The Cu/Se ratio was unrelated to SARS-CoV-2 seropositivity: comparing participants with a Cu/Se ratio above and below the median, the OR was 0.94 [0.44–1.98] ($p = 0.862$), adjusting for household index and smoking. When further adjusting for PFHxS the OR was 0.78 [0.35–1.71] ($p = 0.530$).

Previously identified[22] mixtures of POPs and elements remained substantially associated with SARS-CoV-2 seropositivity when adjusted for any of the PFAS studied. Only PFHxS had a slight influence on our previous estimates of the effect of POPs and elements on seropositivity,[22] with most estimates of the components of the following mixtures increasing modestly: thallium, ruthenium, lead, selenium, and iron (Table 4, model 1); thallium, ruthenium, selenium, and indium (model 2); and gold, lead, and ruthenium (model 3) (again, mutually adjusted, and adjusted for PFHxS and household index). Examples of other mixtures include: thallium, ruthenium, lead, selenium, and DDD (Table 4, model 4, and Figure 2); and thallium, ruthenium, lead, and benzo[b]fluoranthene (model 5). Some components of some mixtures had an OR only >3 or p-values slightly above 0.05; the latter, partly as a result of the numerous covariates and small sample size. Again with different degrees of overlapping, models in Table 4 show the nine exposures that comprised the mixtures more consistently associated with SARS-CoV-2 seropositivity: thallium, ruthenium, lead, benzo[b]fluoranthene, DDD, gold, and (protectively) selenium, indium, and iron.

4. Discussion

No individual PFAS was significantly associated with SARS-CoV-2 seropositivity or COVID-19 disease, and there were no monotonic patterns by quartiles of PFAS concentrations. In addition, PFAS were not confounding our previous estimates[22] of the effect of POPs and chemical elements on the incidence of SARS-CoV-2 seropositivity and COVID-19 disease: several mixtures from three to five POPs and elements remained significantly associated with seropositivity and COVID-19 when adjusted for PFAS, which also did not act as effect modifiers of the mentioned relationships.

More specifically, nine chemicals comprised mixtures associated with COVID-19: thallium, ruthenium, lead, benzo[b]fluoranthene, DDD, other DDT-related compounds, manganese, tantalum, and aluminium. And nine chemicals comprised the mixtures more consistently associated with SARS-CoV-2 seropositivity: thallium, ruthenium, lead, benzo[b]fluoranthene, DDD, gold, and (protectively) selenium, indium, and iron.

Thus, the results suggest that three main types of causal pathways are possible. One path might involve higher concentrations of five substances: thallium, ruthenium, lead, benzo[b]fluoranthene, and DDD, which could increase the risk of both SARS-CoV-2 infection and COVID-19. Another path would involve gold, selenium, indium, and iron, which could increase (and the latter three decrease) the risk of infection, but not so much the risk of COVID-19. And a third type of path would involve manganese, tantalum, aluminium, and DDT-related compounds, which could increase the risk of COVID-19 but not specifically affect the risk of infection.

There are no other studies against which our results on PFAS can be properly compared. For example, the design of a study based on prevalent cases of COVID-19 (in which PFAS were measured in urine samples obtained when participants already had COVID-19) does not allow to state that elevated exposure to PFAS was independently associated with an increased risk of or susceptibility to COVID-19 infection.[26] As mentioned in the Introduction, a relevant difference in time between measurement of the exposures and the outcomes is required to assess whether the contaminants influenced the risk of COVID-19; exposures must be measured clearly before the onset of subclinical disease. We would welcome a study that measured the relevant contaminants closer to the onset of the pandemic, but not too close. Biases due to the use of prevalent cases and cross-sectional designs or to disease progression have long been recognized.[61,62]

In the present study concentrations of PFAS were generally lower than concentrations observed in some studies.[20,51-55] For instance, compared to a study in a sample of the Spanish working / occupied population, we found lower detection frequencies of PFOA, PFDA and PFNA, as well as lower concentrations of these three compounds and of PFOS and PFHxS.[64] Associations between PFAS and

SARS-CoV-2 infection and COVID-19 may exist in populations with higher concentrations and different mixtures of PFAS.

Since PFAS did not increase the risk of SARS-CoV-2 seropositivity or COVID-19 disease, hypotheses on possible mechanisms are not appropriate. The present Introduction provides the rationale for the PFAS analyses; and our previous paper, the rationale and mechanistic hypotheses for the possible effect of POPs and chemical elements on the two outcomes.[22]

In the present study, the Cu/Se ratio was unrelated to the risk of SARS-CoV-2 seropositivity and of developing COVID-19: for participants with a higher Cu/Se ratio, the OR for seropositivity was 0.94 and for COVID-19, 0.60 (both statistically non-significant). In a previous report,[27] the Cu/Se ratio was higher in subjects with severe symptoms of COVID-19 than in subjects with mild symptoms. It is again important to distinguish studies as ours, with the potential to assess etiologic factors, from studies aiming to uncover severity and prognostic markers in inception cohorts of incident cases with early manifestations of the disease.[61,62] The report[27] included prevalent patients with COVID-19 (thus, with no possibility to assess etiologic factors) in a sample of fully-vaccinated health care workers.

Limitations and strengths of the study have been previously discussed.[22] The relatively large number of contaminants analyzed (about 120) enabled a considerable number of comparisons, and it is cogent that we assessed comprehensively their associations with the two outcomes. However, false positives may exist. The size of the study population, the statistical power and precision were often low; yet, numerous effect estimates were precise. Also due to low numbers, we could not assess the association of the contaminants with the severity of the infection and the disease. Our ongoing follow-up and subject accrual will allow to analyze associations of the contaminants with vaccine response and persistent COVID-19.

Conclusions

The PFAS measured were not associated with SARS-CoV-2 seropositivity or COVID-19 disease. The results confirm the associations between personal concentrations of some POPs and chemical elements and SARS-CoV-2 infection and COVID-19 in what so far remains the only prospective and population-based cohort study on the topic. Mixtures of POPs and chemical elements measured at the individual level may contribute to explain the heterogeneity in the risks of SARS-CoV-2 infection and COVID-19 in the general population.

Declaration of competing interests

The authors declare that they have no known competing financial interests or personal relationships that could have appeared to influence the work reported in this paper.

Acknowledgements

The authors gratefully acknowledge technical and scientific assistance provided by the Centre for Genomic Regulation (CRG) Genomics Unit. They also thank Carlo Carolis and Natalia Rodrigo-Melero from CRG for the production of S1 antigen, Luis Izquierdo from ISGlobal for the production of N antigens, and Pere Santamaria, Pau Serra and Daniel Parras from IDIBAPS for the production of S and RBD antigens. Warm thanks are also due to Joan Lop, Marta Pérez, Iris Matilla, Israel Blasco, Alicia Redón, Ana M. Aldea, Núria Somoza, Eulàlia Puigmartí, Carmen Serrano, and Pratima Tamang IMIM PSMar PRBB.

CREDIT AUTHOR STATEMENT

Miquel Porta, Magda Gasull, and José Pumarega conceived the study. Miquel Porta, Magda Gasull, José Pumarega, Luis A. Henríquez-Hernández, Manuel Zumbado, Carlota Dobaño, Gemma Moncunill, Ruth Aguilar, and Cristina Rius obtained funding. Miquel Porta, Magda Gasull, José Pumarega, Carlota Dobaño, Gemma Moncunill, Ruth Aguilar, and Cristina Rius designed the study. Magda Gasull, José Pumarega, Laura Campi, Mar Iglesias, and Pablo Santiago-Díaz conducted field work and follow-up. Jani Koponen, Marta Vidal, Alfons Jimenez, and Manuel Zumbado performed laboratory analyses. Panu Rantakokko, Luis A. Henríquez-Hernández, Ruth Aguilar, Carlota Dobaño, and Gemma Moncunill supervised laboratory analyses. José Pumarega, Magda Gasull, and Laura Campi, did data management. José Pumarega, Magda Gasull, Carolina Donat-Vargas, Laura Campi, and Miquel Porta performed and interpreted statistical analysis. All authors contributed to the interpretation of results. José Pumarega, Miquel Porta, and Magda Gasull drafted the manuscript, and Carolina Donat-Vargas, Luis A. Henríquez-Hernández, Judit Villar-García, Jani Koponen, Ruth Aguilar, Cristina Rius, Carlota Dobaño, and Gemma Moncunill provided additional input. All authors read and approved the final version of the manuscript.

Index of Tables and Figures. By order of appearance in the text.

References

1 Schulz, K., Silva, M.R., Klaper, R., 2020. Distribution and effects of branched versus linear isomers of PFOA, PFOS, and PFHxS: A review of recent literature. Sci Total Environ 733, 139186.

2 Kannan, K., Corsolini, S., Falandysz, J., et al., 2004. Perfluorooctanesulfonate and related fluorochemicals in human blood from several countries. Environ Sci Technol 38, 4489–4495. doi: 10.1021/es0493446.

3 Schneider, J., 2019. PFAS – the 'forever chemicals'. Invisible threats from persistent chemicals. CHEM Trust. https://chemtrust.org/pfasbrief/.

4 Geueke, B., 2016. Dossier: Per- and polyfluoroalkyl substances (PFASs). Zürich: Food Packaging Forum. doi: 10.5281/zenodo.57198. https://www.foodpackagingforum.org/fpf-2016/wp-content/uploads/2016/07/FPF_Dossier10_PFASs.pdf.

5 Gore, A.C., Chappell, V.A., Fenton, S.E., Flaws, J.A., Nadal, A., Prins, G.S., Toppari, J., Zoeller, R.T., 2015. EDC-2: The Endocrine Society's Second Scientific Statement on Endocrine-Disrupting Chemicals. Endocr Rev 36, E1–E150. doi: 10.1210/er.2015-1010.

6 Lim, X., 2023. Could the world go PFAS-free? Proposal to ban 'forever chemicals' fuels debate. Nature 620, 24-27. doi: 10.1038/d41586-023-02444-5.

7 Cousins, I.T., Johansson, J.H., Salter, M.E., Sha, B., Scheringer, M., 2022. Outside the safe operating space of a new planetary boundary for per- and polyfluoroalkyl substances (PFAS). Environ Sci Technol 56, 11172–11179. doi: 10.1021/acs.est.2c02765.

8 Evich, M.G., Davis, M.J.B., McCord, J.P., Acrey, B., Awkerman, J.A., Knappe, D.R.U., Lindstrom, A.B., Speth, T.F., Tebes-Stevens, C., Strynar, M.J., Wang, Z., Weber, E.J., Henderson, W.M., Washington, J.W., 2022. Per- and polyfluoroalkyl substances in the environment. Science, 375 (6580):eabg9065. doi: 10.1126/science.abg9065.

9 Geueke, B., Groh, K.J., Maffini, M.V., Martin, O.V., Boucher, J.M., Chiang, Y.-T., Gwosdz, F., Jieh, P., Kassotis, C.D., Łańska, P., Myers, J.P., Odermatt, A., Parkinson, L.V., Schreier, V.N., Srebny, V., Zimmermann, L., Scheringer, M., Muncke J., 2022. Systematic evidence on migrating and extractable food contact chemicals: Most chemicals detected in food contact materials are not listed for use. Critical Rev Food Sci Nutr, 1-11. https://doi.org/10.1080/10408398.2022.2067828.

10 Scheringer, M., 2023. Innovate beyond PFAS. Science 381, 251–251. https://doi.org/10.1126/science.adj7475.

11 ECHA (European Chemicals Agency), 2023.ECHA publishes PFAS restriction proposal. ECHA/NR/23/04. https://echa.europa.eu/-/echa-publishes-pfas-restriction-proposal.

12 Berg, V., Sandanger, T.M., Hanssen, L., Rylander, C., Nøst, T.H., 2021. Time trends of perfluoroalkyl substances in blood in 30-year old Norwegian men and women in the period 1986-2007. Environ Sci Pollut Res Int 28, 43897–43907.

13 NTP (National Toxicology Program). 2016. Monograph on Immunotoxicity associated with exposure to Perfluorooctanoic acid (PFOA) and Perfluorooctane Sulfonate (PFOS). Washington, DC: National Toxicology Program, U.S. Department of Health and Human Services. Available in: https://ntp.niehs.nih.gov/sites/default/files/ntp/ohat/pfoa_pfos/pfoa_pfosmonograph_508.pdf, and https://www.atsdr.cdc.gov/pfas/health-effects/index.html. Accessed 18 July 2023.

14 DeWitt, J.C., Peden-Adams, M.M., Keller, J.M., Germolec, D.R., 2012. Immunotoxicity of perfluorinated compounds: recent developments. Toxicol Pathol 40, 300-311. doi: 10.1177/0192623311428473.

15 Quinete, N., Hauser-Davis, R.A, 2021. Drinking water pollutants may affect the immune system: concerns regarding COVID-19 health effects. Environ Sci Pollut Res Int, 28: 1235–1246. doi: 10.1007/s11356-020-11487-4.

16 Timmermann, C.A.G., Jensen, K.J., Nielsen, F., et al., 2020. Serum perfluoroalkyl substances, vaccine responses, and morbidity in a cohort of Guinea-Bissau children. Environ Health Perspect 128, 87002. doi: 10.1289/EHP6517.

17 Zhang, X.., Xue, L., Deji, Z., et al., 2022. Effects of exposure to per- and polyfluoroalkyl substances on vaccine antibodies: A systematic review and meta-analysis based on epidemiological studies. Environ Pollut 306, 119442. doi: 10.1016/j.envpol.2022.119442.

18 Grandjean, P., Heilmann, C., Weihe, P., et al., 2017. Estimated exposures to perfluorinated compounds in infancy predict attenuated vaccine antibody concentrations at age 5-years. J Immunotoxicol 14, 188–195.

19 Porter, A.K., Kleinschmidt, S.E., Andres, K.L., et al., 2022. Antibody response to COVID-19 vaccines among workers with a wide range of exposure to per- and polyfluoroalkyl substances. Environ Int 169, 107537. doi: 10.1016/j.envint.2022.107537.

20 Bailey, J.M., Wang, L., McDonald, J.M. et al., 2023. Immune response to COVID-19 vaccination in a population with a history of elevated exposure to per- and polyfluoroalkyl substances (PFAS) through drinking water. J Expo Sci Environ Epidemiol https://doi.org/10.1038/s41370-023-00564-8.

21 Kogevinas, M., Karachaliou, M., Espinosa, A., et al., 2023. Long-term exposure to air pollution and COVID-19 vaccine antibody response in a general population cohort (COVICAT Study, Catalonia). Environ Health Perspect, 131, 47001. doi: 10.1289/EHP11989.

22 Porta, M., Pumarega, J., Gasull, M., et al., 2023. Individual blood concentrations of persistent organic pollutants and chemical elements, and COVID-19: A prospective cohort study in Barcelona. Environ Res 223, 115419.

23 Grandjean, P., Timmermann, C.A.G., Kruse, M., Nielsen, F., Vinholt, P.J., Boding, L., Heilmann, C., Mølbak, K., 2020. Severity of COVID-19 at elevated exposure to perfluorinated alkylates. PLoS One 15, e0244815.

24 Zeng, H.L., Zhang, B., Wang, X., et al., 2021. Urinary trace elements in association with disease severity and outcome in patients with COVID-19. Environ Res 194, 110670.

25 Zeng, H.L., Yang, Q., Yuan, P., et al. 2021. Associations of essential and toxic metals/metalloids in whole blood with both disease severity and mortality in patients with COVID-19. FASEB J 35, e21392.

26 Ji, J., Song, L., Wang, J., et al., 2021. Association between urinary per- and poly-fluoroalkyl substances and COVID-19 susceptibility. Environ Int 153, 106524. https://doi.org/10.1016/j.envint.2021.106524.

27 Tashakori, M., Jamalizadeh, A., Nejad-Ghaderi, M., Hadavi, M., Yousefi-Ahmadipour, A., Moghadam, F.M., Rahnama, M., Haftcheshmeh, S.M., Mashayekhi, K., Momtazi-Borojeni, A.A., 2023. Association between the copper/selenium ratio and the immune response to SARS-CoV-2 infection. Biomark. Med 17, 307-317.

28 Nielsen, C., Jöud, A., 2021. Susceptibility to COVID-19 after High exposure to perfluoroalkyl substances from contaminated drinking water: An ecological study from Ronneby, Sweden. Int. J. Environ. Res. Public Health 18, 10702. https://doi.org/10.3390/ijerph182010702.

29 Catelan, D., Biggeri, A., Russo, F., Gregori, D., Pitter, G., Da Re, F., Fletcher, T., Canova, C., 2021. Exposure to perfluoroalkyl substances and mortality for COVID-19: A spatial ecological analysis in the Veneto Region (Italy). Int. J. Environ. Res. Public Health 18, 2734. https://doi.org/10.3390/ijerph18052734.

30 Karachaliou, M., Moncunill, G., Espinosa, A., et al., 2021. Infection induced SARS-CoV-2 seroprevalence and heterogeneity of antibody responses in a general population cohort study in Catalonia Spain. Scientific Reports 11, 21571.

31 Menges, D., Zens, K.D., Ballouz, T., et al., 2022. Heterogenous humoral and cellular immune responses with distinct trajectories post-SARS-CoV-2 infection in a population-based cohort. Nat Commun 13, 4855. doi: 10.1038/s41467-022-32573-w. https://www.nature.com/articles/s41467-022-32573-w.

32 Le Bert, N., Chia, W.N., Wan, W.Y., et al., 2021. Widely heterogeneous humoral and cellular immunity after mild SARS-CoV-2 infection in a homogeneous population of healthy young men. Emerg Microbes Infect 10, 2141-2150. doi: 10.1080/22221751.2021.1999777. https://doi.org/10.1080/22221751.2021.1999777

33 Mazzoni, A., Maggi, L., Capone, M., et al., 2021. Heterogeneous magnitude of immunological memory to SARS-CoV-2 in recovered individuals. Clin Transl Immunology 10, e1281. doi: 10.1002/cti2.1281. https://doi.org/10.1002/cti2.1281.

34 Kogevinas, M., Castaño-Vinyals, G., Karachaliou, M., et al., 2021. Ambient air pollution in relation to SARS-CoV-2 infection, antibody response, and COVID-19 disease: A cohort study in Catalonia, Spain (COVICAT Study). Environ Health Perspect 129, 117003.

35 Ranzani, O., Alari, A., Olmos, S., et al., 2023. Long-term exposure to air pollution and severe COVID-19 in Catalonia: a population-based cohort study. Nat Commun, 24, 14, 2916. doi: 10.1038/s41467-023-38469-7.

36 Weaver, A.K., Head, J.R., Gould, C.F., Carlton, E.J., Remais, J.V., 2022. Environmental factors influencing COVID-19 incidence and severity. Annu Rev Public Health 43, 271–291.

37 Patanavanich, R., Glantz, S.A., 2021. Smoking is associated with worse outcomes of COVID-19 particularly among younger adults: a systematic review and meta-analysis. BMC Public Health 21, 1554.

38 Dietert, R.R., DeWitt, J.C., Germolec, D.R., Zelikoff, J.T., 2010. Breaking patterns of environmentally influenced disease for health risk reduction: immune perspectives. Environ Health Perspect 118, 1091–1099.

39 Germolec, D.R., Lebrec, H., Anderson, S.E., et al., 2022. Consensus on the key characteristics of immunotoxic agents as a basis for hazard identification. Environ Health Perspect 130, 105001.

40 Bulka, C.M., Enggasser, A.E., Fry, R.C., 2022. Epigenetics at the intersection of COVID-19 risk and environmental chemical exposures. Curr Environ Health Rep 9, 477–489.

41 Kostoff, R.N., Briggs, M.B., Kanduc, D., et al., 2023. Modifiable contributing factors to COVID-19: A comprehensive review. Food Chem Toxicol 171, 113511. doi: 10.1016/j.fct.2022.113511.

42 Pagano, G., Aliberti, F., Guida, M. et al., 2015. Rare earth elements in human and animal health: state of art and research priorities. Environ Res 142, 215–220.

43 Agency for Toxic Substances and Disease Registry (ATSDR). ATSDR 2019 Substance Priority List. Available in: https://www.atsdr.cdc.gov/spl/index.html. Accessed 18 July 2023.

44 Henríquez-Hernández, L.A., Boada, L.D., Carranza, C., et al., 2017. Blood levels of toxic metals and rare earth elements commonly found in e-waste may exert subtle effects on hemoglobin concentration in sub-Saharan immigrants. Environ Int 109, 20–28.

45 Porta, M., Pumarega, J., Henríquez-Hernández, L.A., et al., 2021. Reductions in blood concentrations of persistent organic pollutants in the general population of Barcelona from 2006 to 2016. Sci Total Environ 777, 146013.

46 Porta, M., López, T., Gasull, M., et al., 2012. Distribution of blood concentrations of persistent organic pollutants in a representative sample of the population of Barcelona in 2006, and comparison with levels in 2002. Sci Total Environ 423, 151–161.

47 Porta, M., Gasull, M., Puigdomènech, E., et al., 2009. Sociodemographic factors influencing participation in the Barcelona Health Survey study on serum concentrations of persistent organic pollutants. Chemosphere 76, 216–225.

48 Dobaño, C., Vidal, M., Santano, R., et al., 2020. Highly sensitive and specific multiplex antibody assays to quantify immunoglobulins M, A, and G against SARS-CoV-2 antigens. J Clin Microbiol 59, e01731.

49 World Health Organization (WHO). Public health surveillance for COVID-19 Interim guidance. 14 February 2022. WHO reference number: WHO/2019-nCoV/SurveillanceGuidance/2022.1. Available at: https://www.who.int/publications/i/item/WHO-2019-nCoV-SurveillanceGuidance-2022.1. Accessed 18 July 2023.

50 Koponen, J., Rantakokko, P., Airaksinen, R., Kiviranta, H., 2013. Determination of selected perfluorinated alkyl acids and persistent organic pollutants from a small volume human serum sample relevant for epidemiological studies. J Chromatogr A 1309, 48–55.

51 Haines, D.A., Saravanabhavan, G., Werry, K., Khoury, C., 2017. An overview of human biomonitoring of environmental chemicals in the Canadian Health Measures Survey: 2007-2019. Int J Hyg Environ Health 220, 13–28.

52. Haines, D.A., Arbuckle, T.E., Lye, E., Legrand, M., Fisher, M., Langlois, R., Fraser, W., 2011. Reporting results of human biomonitoring of environmental chemicals to study participants: a comparison of approaches followed in two Canadian studies. J Epidemiol Community Health, 65, 191–198.

53 Centers for Disease Control and Prevention, 2022. National Report on Human Exposure to Environmental Chemicals; Atlanta, GA. https://www.cdc.gov/exposurereport/report/pdf/Perfluoroalkyl%20and%20Polyfluoroalkyl%20Substances%20--%20Surfactants%20NHANES-p.pdf, and https://www.cdc.gov/exposurereport/index.html. Accessed 18 July 2023.

54 Colles, A., Bruckers, L., Den Hond, E., Govarts, E., Morrens, B., Schettgen, T., Buekers, J., Coertjens, D., Nawrot, T., Loots, I., Nelen, V., De Henauw, S., Schoeters, G., Baeyens, W., van Larebeke, N., 2020. Perfluorinated substances in the Flemish population (Belgium): Levels and determinants of variability in exposure. Chemosphere 242, 125250.

55 Fillol, C., Oleko, A., Saoudi, A., Zeghnoun, A., Balicco, A., Gane, J., Rambaud, L., Leblanc, A., Gaudreau, É., Marchand, P., Le Bizec, B., Bouchart, V., Le Gléau, F., Durand, G., Denys, S., 2021. Exposure of the French population to bisphenols, phthalates, parabens, glycol ethers, brominated flame retardants, and perfluorinated compounds in 2014-2016: Results from the Esteban study. Environ Int 147, 106340. doi: 10.1016/j.envint.2020.106340.

56 Henríquez-Hernández, L.A., Luzardo, O.P., Zumbado, M., Serra-Majem, L., Valerón, P.F., Camacho, M., Álvarez-Pérez, J., Salas-Salvadó, J., Boada, L.D., 2017. Determinants of increasing serum POPs in a population at high risk for cardiovascular disease. Results from the PREDIMED-CANARIAS study. Environ Res 156, 477–484. doi: 10.1016/j.envres.2017.03.053.

57 Luzardo, O.P., Badea, M., Zumbado, M., Rogozea, L., Floroian, L., Ilea, A., Moga, M., Sechel, G., Boada, L.D., Henríquez-Hernández, LA., 2019. Body burden of organohalogenated pollutants and polycyclic aromatic hydrocarbons in Romanian population: Influence of age, gender, body mass index, and habitat. Sci Total Environ 656, 709–716. doi: 10.1016/j.scitotenv.2018.11.404.

58 González-Antuña, A., Camacho, M., Henríquez-Hernández, L.A., Boada, L.D., Almeida-González, M., Zumbado, M., Luzardo, O.P., 2017. Simultaneous quantification of 49 elements associated to e-waste in human blood by ICP-MS for routine analysis. MethodsX 4, 328–334. doi: 10.1016/j.mex.2017.10.001.

59 Henríquez-Hernández, L.A., Romero, D., González-Antuña, A., Gonzalez-Alzaga, B., Zumbado, M., Boada, L.D., Hernández, A.F., López-Flores, I., Luzardo, O.P., Lacasaña, M., 2020. Biomonitoring of 45 inorganic elements measured in plasma from Spanish subjects: A cross-sectional study in Andalusian population. Sci Total Environ 706, 135750. doi: 10.1016/j.scitotenv.2019.135750.

60 Cabrera-Rodríguez, R., Luzardo, O.P., Almeida-González, M., Boada, L.D., Zumbado, M., Acosta-Dacal, A., Rial-Berriel, C., Henríquez-Hernández, L.A., 2019. Association between prenatal exposure to multiple persistent organic pollutants (POPs) and growth indicators in newborns. Environ Res 171, 285–292. doi: 10.1016/j.envres.2018.12.064.

61 Lash, T.L., VanderWeele, T.J., Haneuse, S., Rothman, K.J., (Eds.), 2021. Modern epidemiology. 4th. ed., Philadelphia: Wolters-Kluwer.

62 Porta, M., Greenland, S., Hernán, M., dos Santos Silva, I., Last, M., (Eds.), 2014. A dictionary of epidemiology. 6th. edition. New York: Oxford University Press and International Epidemiological Association: pp. 261–262.

63 Carrico, C., Gennings, C., Wheeler, D.C., Factor-Litvak, P., 2015. Characterization of weighted quantile sum regression for highly correlated data in a risk analysis setting. J Agric Biol Environ Stat 20, 100–120.

64 Bartolomé, M., Gallego-Picó, A., Cutanda, F., Huetos, O., Esteban, M., Pérez-Gómez, B.; Bioambient.es; Castaño A. 2017. Perfluorinated alkyl substances in Spanish adults: Geographical distribution and determinants of exposure. Sci Total Environ 603-604, 352–360.

Table 1. Association of per- and polyfluoroalkyl substances (PFAS) with COVID-19. Single pollutant models (N = 154).*

PFAS	OR[a]	(95% CI)	P[b]
PFOA			
Q1	1.00		0.680
Q2	2.48	(0.55 -11.13)	
Q3	1.69	(0.36 -7.99)	
Q4	1.50	(0.31 -7.36)	
Q1	1.00		0.357
≥Q2	1.87	(0.49 -7.06)	
PFDA			
Q1+Q2[c]	1.00		0.136
Q3	0.17	(0.02 -1.39)	
Q4	1.65	(0.50 -5.40)	
≤Q3	1.00		0.155
Q4	2.32	(0.73 -7.41)	
PFNA			
Q1	1.00		0.927
Q2	0.64	(0.16 -2.58)	
Q3	0.71	(0.17 -2.92)	
Q4	0.74	(0.18 -3.00)	
Q1	1.00		0.512
≥Q2	0.69	(0.23 -2.06)	
PFUnDA			
Q1+Q2[c]	1.00		0.437
Q3	0.44	(0.11 -1.80)	
Q4	1.24	(0.37 -4.12)	
≤Q3	1.00		0.431
Q4	1.58	(0.50 -4.98)	
PFHxS			
Q1	1.00		0.373
Q2	0.45	(0.11 -1.74)	
Q3	0.58	(0.15 -2.21)	
Q4	0.25	(0.05 -1.29)	
Q1	1.00		0.131
≥Q2	0.43	(0.14 -1.29)	
PFOS total			
Q1	1.00		0.802
Q2	0.48	(0.10 -2.19)	
Q3	0.92	(0.24 -3.46)	
Q4	0.74	(0.18 -3.06)	
Q1	1.00		0.540
≥Q2	0.71	(0.23 -2.14)	
continuous[d]	0.76	(0.13 -4.58)	0.769
PFOS linear			
Q1	1.00		0.979
Q2	1.07	(0.26 -4.42)	
Q3	1.15	(0.26 -5.06)	
Q4	1.34	(0.32 -5.58)	
Q1	1.00		0.787
≥Q2	1.18	(0.36 -3.82)	
continuous[d]	0.89	(0.15 -5.39)	0.899

[continued]

Table 1. Continued.

PFAS	OR[a]	(95% CI)	P[b]
PFOS branched			
Q1[c]	1.00		0.352
Q2	0.66	(0.18 -2.38)	
Q3	0.57	(0.15 -2.12)	
Q4	0.21	(0.04 -1.16)	
Q1[c]	1.00		0.097
≥Q2	0.66	(0.41 -1.08)	
continuous[d]	0.40	(0.12 -1.32)	0.132
Sum conc. of 5 PFAS[e]			
Q1	1.00		0.635
Q2	1.23	(0.33 -4.60)	
Q3	0.48	(0.10 -2.28)	
Q4	1.15	(0.25 -5.19)	
Q1+Q2	1.00		0.400
Q3+Q4	0.64	(0.23 -1.80)	
continuous[d]	0.79	(0.10 -6.28)	0.825
Sum of orders of 7 PFAS[f]			
Q1	1.00		0.574
Q2	0.61	(0.15 -2.50)	
Q3	0.39	(0.09 -1.72)	
Q4	0.98	(0.25 -3.87)	
≤Q3	1.00		0.481
Q4	1.53	(0.47 -4.95)	

* The odds ratios quantify the magnitude of the associations between the exposures and COVID-19 disease in the 154 individuals, 20 with COVID-19 and 134 without the disease. An odds ratio of 1.00 denotes the reference category.

[a] Odds ratios adjusted for age, education and smoking.
[b] Wald's test.
[c] The category is exclusively made up of individuals whose the corresponding PFAS concentration could not be quantified.
[d] Odds ratio for each increase of 10 times in the concentration (ng/mL).
[e] Sum of concentrations (ng/mL) of PFOA, PFDA, PFNA, PFUnDA, and PFHxS, and categorized in quartiles.
[f] Sum of rank of quartiles of PFOA, PFDA, PFNA, PFUnDA, PFHxS, PFOS linear, and PFOS branched, and categorized in quartiles.

Table 2. Association of mixtures of POPs and elements with COVID-19, adjusting for PFOS branched (N = 154).*

Model[a]		OR[b]	(95% CI)	P[c]	Model[a]	OR[b]	(95% CI)	P[c]
1a	***p,p'*-DDD**				**1b**			
	Not detected	1.00		0.003		—		
	Detected	120.9	(5.22 -2803)					
	Manganese							
	Not detected	1.00		0.027		1.00		0.031
	Detected	12.81	(1.34 -141.9)			11.55	(1.25 -106.8)	
	Ruthenium							
	Not detected	1.00		0.016		1.00		0.021
	Detected	4.80	(1.33 -17.31)			3.87	(1.22 -12.23)	
	Tantalum							
	Not detected	1.00		0.008		1.00		0.028
	Detected	7.63	(1.72 -33.91)			4.42	(1.17 -16.68)	
2a	***p,p'*-DDD**				**2b**			
	Not detected	1.00		0.005		—		
	Detected	193.4	(5.09 -7354)					
	Ruthenium							
	Not detected	1.00		0.003		1.00		0.004
	Detected	6.53	(1.87 -22.88)			5.17	(1.67 -15.99)	
	Lead							
	≤Q3	1.00		0.007		1.00		0.016
	Q4	9.96	(1.87 -53.10)			5.79	(1.39 -24.17)	
3a	***p,p'*-DDE**				**3b**			
	≤Q3	1.00		0.032		1.00		0.074
	Q4	5.80	(1.16 -29.00)			4.67	(0.86 -25.27)	
	Manganese							
	Not detected	1.00		0.024		1.00		0.020
	Detected	13.55	(1.41 -129.8)			17.79	(1.57 -201.3)	
	Benzo[b]fluoranthene							
	Not detected	—				1.00		0.025
	Detected					51.06	(1.66 -1576)	
	Tantalum							
	Not detected	1.00		0.025		1.00		0.015
	Detected	4.43	(1.21 -16.27)			5.36	(1.39 -20.74)	
4a	***p,p'*-DDT**				**4b**			
	Not detected	1.00		0.108		1.00		0.069
	Detected	7.22	(0.65 -80.22)			11.04	(0.83 -147.2)	
	Ruthenium							
	Not detected	1.00		0.006		1.00		0.005
	Detected	5.46	(1.63 -18.26)			6.72	(1.79 -25.29)	
	Lead							
	≤Q3	1.00		0.007		1.00		0.006
	Q4	8.49	(1.77 -40.70)			11.97	(2.05 -70.07)	
	Thallium							
	Q1+Q2	1.00		0.027		1.00		0.018
	Q3+Q4	5.18	(1.20 -22.27)			6.43	(1.37 -30.10)	
	Benzo[b]fluoranthene							
	Not detected	—				1.00		0.006
	Detected					50.39	(3.11 -815.8)	

[continued]

Table 2, continued.

Model[a]		OR[b]	(95% CI)	P[c]	Model[a]	OR[b]	(95% CI)	P[c]
5a	**Ruthenium**				**5b**			
	Not detected	1.00		0.005		1.00		0.009
	Detected	6.44	(1.76 -23.54)			6.00	(1.55 -23.19)	
	Lead							
	≤Q3	1.00		0.008		1.00		0.012
	Q4	10.34	(1.83 -58.37)			9.78	(1.65 -57.96)	
	Thallium							
	Q1+Q2	1.00		0.020		1.00		0.035
	Q3+Q4	6.00	(1.33 -27.13)			5.46	(1.13 -26.31)	
	Manganese							
	Not detected	—				1.00		0.111
	Detected					8.09	(0.62 -105.5)	
	Benzo[b]fluoranthene							
	Not detected	1.00		0.008		1.00		0.008
	Detected	39.39	(2.64 -586.9)			58.72	(2.93 -1176)	
6a	**Sum of DDT, DDD and DDE[d]**				**6b**			
	Low	1.00		0.036		1.00		0.081
	High	5.57	(1.12 -27.77)			4.50	(0.83 -24.29)	
	Manganese							
	Not detected	1.00		0.024		1.00		0.020
	Detected	13.58	(1.42 -130.2)			17.93	(1.58 -203.7)	
	Benzo[b]fluoranthene							
	Not detected	—				1.00		0.024
	Detected					51.37	(1.69 -1559)	
	Tantalum							
	Not detected	1.00		0.024		1.00		0.014
	Detected	4.49	(1.22 -16.49)			5.42	(1.40 -20.98)	
7a	**Manganese**				**7b**			
	Not detected	1.00		0.019		1.00		0.021
	Detected	18.93	(1.63 -220.3)			19.50	(1.56 -244.2)	
	Benzo[b]fluoranthene							
	Not detected	1.00		0.009		1.00		0.004
	Detected	61.90	(2.84 -1349)			108.6	(4.46 -2642)	
	Tantalum							
	Not detected	1.00		0.020		1.00		0.014
	Detected	4.83	(1.28 -18.15)			5.65	(1.41 -22.62)	
	Aluminium							
	Not detected	—				1.00		0.016
	Detected					14.97	(1.65 -136.2)	
8	**Manganese**				**9**			
	Not detected	1.00		0.029		—		
	Detected	11.57	(1.28 -104.8)					
	Tantalum							
	Not detected	1.00		0.030		—		
	Detected	4.18	(1.15 -15.15)					
	Aluminium							
	Not detected	1.00		0.046		1.00		0.045
	Detected	8.13	(1.04 -63.91)			10.08	(1.05 -96.63)	
	Ruthenium							
	Not detected	—				1.00		0.032
	Detected					3.51	(1.12 -11.04)	
	Benzo[b]fluoranthene							
	Not detected	—				1.00		0.007
	Detected					38.72	(2.67 -562.3)	

*The odds ratios (ORs) quantify the magnitude of the associations between the exposures and COVID-19 in the 154 individuals, 20 with COVID-19 and 134 without the disease (see Methods section). An OR of 1.00 denotes the reference category.

[a] Cut-off points of the concentrations for the exposure categories (quartiles, limits of detection and quantification) are shown in Porta et al., 2023 (Supplemental Table 2). Model 1a relates to model 1 (the latter, unadjusted for PFOS branched) of Table 3 of Porta et al., 2023; model 2a relates to model 3 of the same Table; model 3a, to model 4; model 4a, to model 5; and model 6a, to model 6 of the same Table 3 of Porta et al., 2023.

[b] Odds ratios of the chemicals are always mutually adjusted for, and further adjusted by PFOS branched (continuous, and not significantly associated with COVID-19 in any model), as well as by age, education and smoking (all three confounders $p<0.25$ or ~0.25, see Methods, section 2.6).

[c] Wald's test (two-tailed).

[d] When an individual had DDT and/or DDD detected, and/or DDE in the upper quartile, he was classified as 'high'; when DDT and DDD were not detected and DDE was in any of the 3 lower quartiles, the individual was classified as 'low' (Porta et al., 2023).

Table 3. Association of per- and polyfluoroalkyl substances (PFAS) with SARS-CoV-2 seropositivity. Single pollutant models (N = 145).*

PFAS	OR[a]	(95% CI)	P[b]
PFOA			
Q1	1.00		0.581
Q2	1.71	(0.59 -4.91)	
Q3	1.14	(0.38 -3.38)	
Q4	0.84	(0.27 -2.58)	
≤Q3	1.00		0.368
Q4	0.66	(0.27 -1.63)	
PFDA			
≤Q3	1.00		0.678
Q4	1.21	(0.50 -2.91)	
PFNA			
Q1	1.00		0.776
Q2	1.00	(0.36 -2.80)	
Q3	0.62	(0.21 -1.80)	
Q4	0.72	(0.25 -2.10)	
Q1+Q2	1.00		0.306
Q3+Q4	0.67	(0.31 -1.45)	
PFUnDA			
Q1+Q2[c]	1.00		0.323
Q3	0.47	(0.17 -1.29)	
Q4	0.92	(0.37 -2.27)	
PFHxS			
Q1	1.00		0.126
Q2	0.35	(0.12 -1.00)	
Q3	0.58	(0.21 -1.63)	
Q4	0.31	(0.10 -0.96)	
Q1	1.00		0.035
≥Q2	0.40	(0.17 -0.94)	
continuous[d]	0.44	(0.16 -1.18)	0.102
PFOS total			
Q1	1.00		0.648
≥Q2	0.82	(0.35 -1.91)	
continuous[d]	0.49	(0.13 -1.85)	0.294
PFOS linear			
Q1	1.00		0.872
Q2	1.04	(0.36 -2.97)	
Q3	0.86	(0.29 -2.54)	
Q4	0.69	(0.23 -2.08)	
≤Q3	1.00		0.451
Q4	0.71	(0.29 -1.73)	
continuous[d]	0.52	(0.14 -1.95)	0.329

[continued]

Table 3, continued.

PFAS	OR[a]	(95% CI)	P[b]
PFOS branched			
Q1	1.00		0.510
Q2	0.73	(0.27 -2.03)	
Q3	0.43	(0.14 -1.29)	
Q4	0.64	(0.21 -1.90)	
Q1	1.00		0.233
≥Q2	0.59	(0.25 -1.40)	
continuous[d]	0.58	(0.24 -1.42)	0.231
Sum of concentr. of 5 PFAS[e]			
Q1	1.00		0.356
Q2	0.82	(0.29 -2.34)	
Q3	0.38	(0.13 -1.18)	
Q4	0.58	(0.18 -1.83)	
Q1+Q2	1.00		0.099
Q3+Q4	0.52	(0.24 -1.13)	
continuous[d]	0.45	(0.10 -2.04)	0.298
Sum of orders of 7 PFAS[f]			
Q1	1.00		0.481
Q2	0.71	(0.24 -2.05)	
Q3	0.43	(0.14 -1.30)	
Q4	0.87	(0.29 -2.60)	
Q1	1.00		0.290
≥Q2	0.63	(0.26 -1.49)	

* The odds ratios quantify the magnitude of the associations between the exposures and SARS-CoV-2 seropositivity in the 145 individuals, 41 SARS-CoV-2 seropositives and the 104 seronegatives. See also footnotes in Table 1.

[a] Unless otherwise specified, odds ratios were adjusted for household outdoor index and smoking.

[b] Wald's test.

[c] The category is exclusively made up of individuals whose the corresponding PFAS concentration could not be quantified.

[d] Odds ratio for each increase of 10 times in the concentration (ng/mL).

[e] Sum of concentrations of PFOA, PFDA, PFNA, PFUnDA, and PFHxS (ng/mL), and categorized in quartiles.

[f] Sum of rank of quartiles of PFOA, PFDA, PFNA, PFUnDA, PFHxS, PFOS linear, and PFOS branched, and categorized in quartiles.

Table 4. Association of mixtures of POPs and elements with SARS-CoV-2 seropositivity, adjusting for PFHxS (N = 145).*

Model[a]		OR[b]	(95% CI)	P[c]
1	**Thallium**			
	Q1+Q2	1.00		<0.001
	Q3+Q4	5.39	(2.13 -15.24)	
	Ruthenium			
	Not detected	1.00		0.005
	Detected	3.78	(1.51 -9.89)	
	Lead			
	≤Q3	1.00	(1.39 -11.92)	0.011
	Q4	3.95		
	Selenium			
	≤Q3	1.00		0.025
	Q4	0.28	(0.08 -0.80)	
	Iron			
	Q4	1.00		0.054
	≤Q3	3.34	(0.98 -11.36)	
2	**Thallium**			
	Q1+Q2	1.00		<0.001
	Q3+Q4	6.27	(2.50 -17.55)	
	Ruthenium			
	Not detected	1.00		0.002
	Detected	4.40	(1.73 -11.85)	
	Selenium			
	≤Q3	1.00		0.020
	Q4	0.28	(0.09 -0.77)	
	Indium			
	Not detected	1.00		0.021
	Detected	0.28	(0.09 -0.79)	
3	**Gold**			
	Not detected	1.00		0.039
	Detected	2.33	(1.05 -5.29)	
	Lead			
	≤Q3	1.00		0.030
	Q4	2.98	(1.12 -8.16)	
	Ruthenium			
	Not detected	1.00		
	Detected	2.76	(1.17 -6.58)	0.021

[continued]

Table 4, continued.

Model[a]		OR[b]	(95% CI)	P[c]
4	**Thallium**			
	Q1+Q2	1.00		<0.001
	Q3+Q4	5.61	(2.13 -14.81)	
	Ruthenium			
	Not detected	1.00		0.007
	Detected	3.66	(1.44 -9.33)	
	Lead			
	≤Q3	1.00		0.020
	Q4	3.55	(1.22 -10.34)	
	Selenium			
	≤Q3	1.00		0.012
	Q4	0.24	(0.08 -0.74)	
	***p,p'*-DDD**			
	Not detected	1.00		0.097
	Detected	9.48	(0.66 -135.4)	
5	**Thallium**			
	Q1+Q2	1.00		0.001
	Q3+Q4	4.43	(1.78 -11.00)	
	Ruthenium			0.009
	Not detected	1.00		
	Detected	3.29	(1.35 -8.01)	
	Lead			
	≤Q3	1.00		0.073
	Q4	2.51	(0.92 -6.87)	
	Benzo[b]fluoranthene			
	Not detected	1.00		0.144
	Detected	5.86	(0.55 -62.74)	

*The odds ratios quantify the magnitude of the associations between the exposures and SARS-CoV-2 seropositivity in the 145 individuals, 41 SARS-CoV-2 seropositives and 104 seronegatives (see Supplemental Table 5). An OR of 1.00 denotes the reference category.

[a] Cut-off points of the concentrations for the exposure categories (quartiles, limits of detection and quantification) are shown in Porta et al., 2023. Models 1 to 3 relate to models 1 to 3 (the latter, unadjusted for PFHxS) of Table 5 of Porta et al., 2023.

[b] Odds ratios of the chemicals were mutually adjusted for, and further adjusted by PFHxS (continuous), as well as by household outdoor index ($p<0.25$ or ~0.25, see Methods section 2.6). The odds ratios of all chemicals have a p-value <0.15 (see also Methods, section 2.6).

[c] Wald's test.

Figure 1. Forest plot of associations of DDT, ruthenium, lead, thallium, and benzo[b]fluoranthene with COVID-19 when adjusting for PFOS branched.

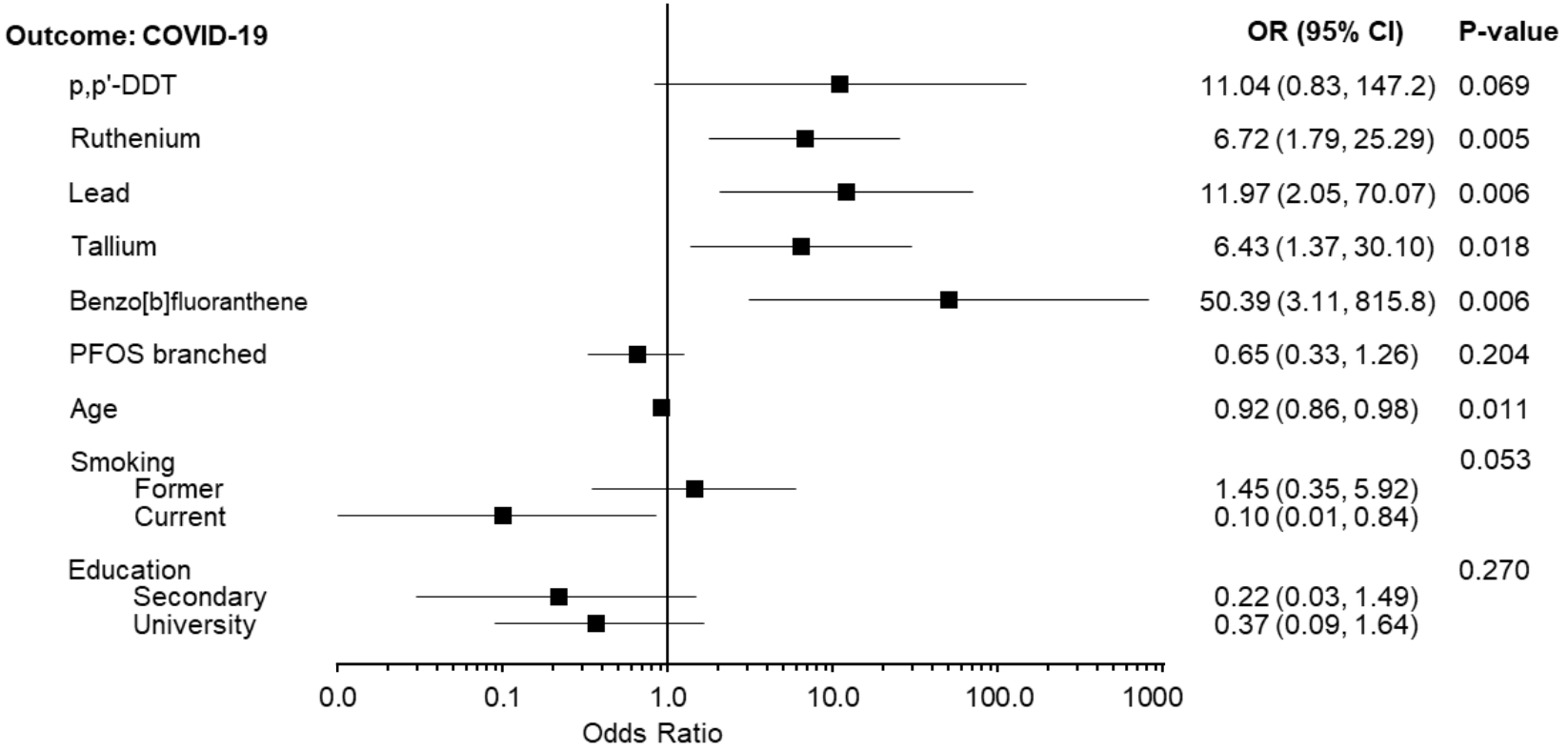

Figure 2. Forest plot of associations of DDD, thallium, ruthenium, lead, and selenium with SARS-CoV-2 seropositivity when adjusting for PFHxS.

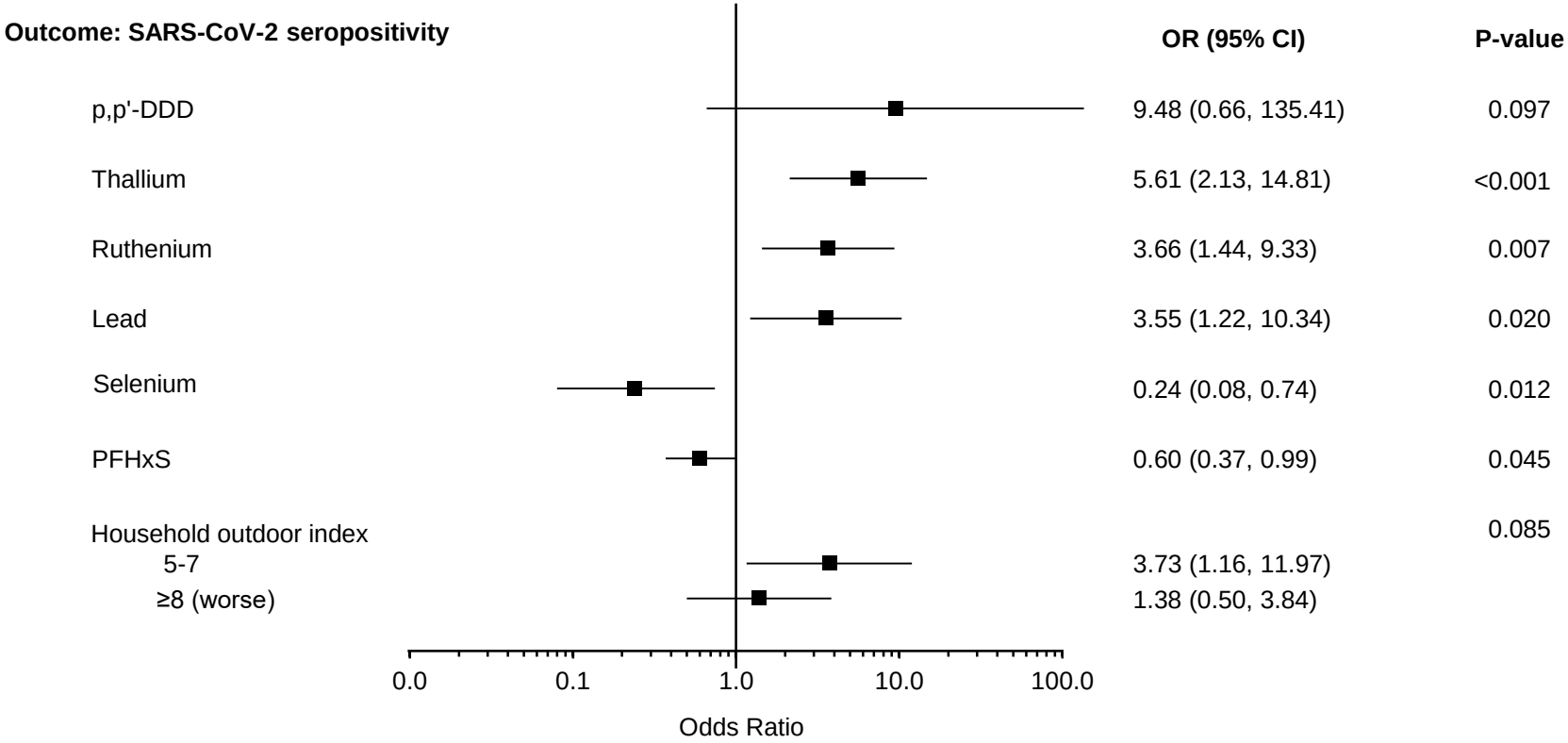

Supplemental Table 1. Limit of quantification, percentage of participants with concentrations of per- and polyfluoroalkyl substances (PFAS) above the limit, and concentrations (ng/mL) observed in the study participants (N=240).

Per- and polyfluoroalkyl substances in 2016-2017	LOQ	Percent ≥LOQ	GM	P25	P50	P75
PFOA	0.018	98.8	1.26	0.89	1.33	2.01
PFDA	0.018	45.0	0.16	<LOQ	<LOQ	0.29
PFNA	0.018	92.5	0.54	0.41	0.59	0.86
PFUnDA	0.018	55.4	0.19	<LOQ	0.20	0.38
PFHxS	0.018	86.7	0.50	0.31	0.61	0.97
PFOS total	0.018	100.0	3.93	2.69	4.25	6.07
PFOS linear	0.018	100.0	3.45	2.41	3.58	5.27
PFOS branched	0.018	76.3	0.38	0.19	0.41	0.83

LOQ: limit of quantification.
GM: geometric mean. P25: percentile 25th. P50: percentile 50th (median). P75: percentile 75th.
The LOQs, geometric means, and percentiles are expressed in ng/mL.

Supplemental Table 2. Percentage of quantification and concentrations of per- and polyfluoroalkyl substances (ng/mL) in participants included and excluded in the study (N=240).

Per- and polyfluoroalkyl substances in 2016-17	Included	Excluded	P
Number of subjects (%)	174 (72.5)	66 (27.5)	
PFOA n (% quantification)	172 (98.9)	65 (98.5)	>0.999 [a]
Geometric mean (ng/mL)	1.29	1.19	0.775 [b]
(95% CI)	(1.17-1.42)	(0.99-1.43)	
Median	1.34	1.29	0.699 [c]
PFDA n (% quantification)	83 (47.7)	25 (37.9)	0.193 [a]
Geometric mean (ng/mL)	0.16	0.16	0.546 [b]
(95% CI)	(0.14-0.18)	(0.13-0.19)	
Median	0.09	0.09	0.796 [c]
PFNA n (% quantification)	164 (94.3)	58 (87.9)	0.105 [a]
Geometric mean (ng/mL)	0.56	0.50	0.932 [b]
(95% CI)	(0.51-0.62)	(0.41-0.62)	
Median	0.60	0.59	0.675 [c]
PFUnDA n (% quantification)	97 (55.7)	36 (54.5)	0.979 [a]
Geometric mean (ng/mL)	0.19	0.19	0.777 [b]
(95% CI)	(0.17-0.22)	(0.15-0.23)	
Median	0.20	0.19	0.669 [c]
PFHxS n (% quantification)	151 (86.8)	57 (86.4)	>0.999 [a]
Geometric mean (ng/mL)	0.49	0.52	0.581 [b]
(95% CI)	(0.43-0.56)	(0.42-0.65)	
Median	0.61	0.75	0.499 [c]
PFOS total n (% quantification)	174 (100)	66 (100)	[a]
Geometric mean (ng/mL)	3.92	3.95	0.389 [b]
(95% CI)	(3.56-4.32)	(3.25-4.80)	
Median	4.25	4.26	0.766 [c]
PFOS linear n (% quantification)	174 (100)	66 (100)	[a]
Geometric mean (ng/mL)	3.44	3.48	0.380 [b]
(95% CI)	(3.13-3.79)	(2.88-4.21)	
Median	3.58	3.61	0.799 [c]
PFOS branched n (% quantification)	134 (77.0)	49 (74.2)	0.734 [a]
Geometric mean (ng/mL)	0.38	0.37	0.676 [b]
(95% CI)	(0.33-0.44)	(0.28-0.48)	
Median	0.41	0.40	0.855 [c]

% quantification: percentage of individuals with a concentration above the limit of quantification.
[a] Fisher's exact test (two-tail).
[b] Student's *t*-test (two-tail).
[c] Mann-Whitney's *U* test (two-tail).

Supplemental Table 3. Spearman's correlation coefficients between concentrations of PFAS.

Spearman's rho (ρ)		PFOA	PFDA	PFNA	PFUnDA	PFHxS	PFOS linear
PFDA	ρ	0.553					
PFNA	ρ	0.753	0.757				
PFUnDA	ρ	0.496	0.785	0.734			
PFHxS	ρ	0.599	0.410	0.570	0.419		
PFOS total	ρ	0.706	0.722	0.813	0.700	0.691	
PFOS linear	ρ	0.688	0.727	0.789	0.732	0.642	
PFOS branched	ρ	0.411	0.330	0.523	0.221	0.512	0.421

N = 240. ρ = rho coefficient of Spearman's correlation.
Concentrations in ng/mL.
All p-values <0.001.

Supplemental Table 4. Association of POPs and elements with COVID-19 when adjusting for PFOS branched. (N = 154).*

Chemical[a]	OR[b]	(95% CI)	P[c]
***p,p'*-DDT**			
Not detected	1.00		0.163
Detected	4.55	(0.54 -38.25)	
***p,p'*-DDE**			
≤Q3	1.00		0.036
Q4	5.06	(1.11 -23.01)	
***p,p'*-DDD**			
Not detected	1.00		0.008
Detected	54.35	(2.79 -1059)	
Sum of DDT, DDD and DDE[d]			
Low	1.00		0.042
High	4.78	(1.06 -21.55)	
HCB[e]			
Q1	1.00		0.675
≥Q2	1.31	(0.38 -4.54)	
PCB 153			
Q1	1.00		0.750
Q2	1.79	(0.43 -7.45)	
Q3	1.69	(0.30 -9.46)	
Q4	2.91	(0.41 -20.68)	
PCB 180			
Q1	1.00		0.722
Q2	1.53	(0.36 -6.58)	
Q3	1.31	(0.19 -8.93)	
Q4	2.81	(0.39 -20.46)	
Sum of orders of PCBs 138-153-180[e,f]			
Q1	1.00		0.362
Q2	1.81	(0.45 -7.23)	
Q3	1.24	(0.21 -7.26)	
Q4	4.28	(0.66 -27.83)	
≤Q3	1.00		0.112
Q4	3.00	(0.78 -11.57)	
Sum of PCBs 138-153-180[e,g]			
Q1	1.00		0.241
Q2	2.72	(0.67 -11.15)	
Q3	1.53	(0.23 -9.64)	
Q4	5.25	(0.70 -35.42)	
Q1	1.00		0.187
≥Q2	2.49	(0.64 -9.63)	
PCB 126			
Not detected	1.00		0.276
Detected	4.18	(0.32 -54.74)	
PCB 157			
Not quantified	1.00		0.205
Quantified	3.69	(0.49 -27.81)	
Naphthalene			
Q1	1.00		0.602 [h]
Q2	1.01	(0.20 -5.22)	
Q3	1.38	(0.31 -6.22)	
Q4	1.67	(0.38 -7.40)	
Phenanthrene[i]			
Q1	1.00		0.325
Q2	1.33	(0.27 -6.58)	
Q3	1.25	(0.24 -6.40)	
Q4	3.28	(0.75 -14.35)	

[continued]

Supplemental Table 4. Continued.

Chemical[a]	OR[b]	(95% CI)	P[c]
Pyrene[i]			
Q1	1.00		0.167
Q2	2.93	(0.53 -16.38)	
Q3	2.37	(0.39 -14.47)	
Q4	4.63	(0.85 -25.28)	
Fluoranthene			
Q1	1.00		0.264
Q2	4.04	(0.74 -22.00)	
Q3	1.43	(0.21 -9.71)	
Q4	3.43	(0.60 -19.51)	
BDE 153			
Not quantified	1.00		0.156
Quantified	2.73	(0.68 -10.97)	
Benzo(b)fluoranthene			
Not detected	1.00		0.012
Detected	23.84	(2.01 -283.1)	
Indene(123,cd)pyrene			
Not detected	1.00		0.361
Detected	3.94	(0.21 -75.07)	
Lead			
Q1	1.00		0.244
Q2	0.81	(0.18 -3.60)	
Q3	0.86	(0.16 -4.76)	
Q4	3.35	(0.60 -18.85)	
≤Q3	1.00		0.043
Q4	3.90	(1.04 -14.59)	
Continuous[j]	8.59	(1.10 -67.27)	0.041
Arsenic[k]			
Q1	1.00		0.933
Q2	1.47	(0.36 -5.94)	
Q3	1.40	(0.37 -5.34)	
Q4	1.10	(0.25 -4.89)	
Cadmium			
Q1	1.00		0.846
Q2	1.27	(0.32 -5.01)	
Q3	0.60	(0.12 -2.86)	
Q4	0.92	(0.21 -4.04)	
Mercury			
Q1	1.00		0.175
Q2	1.02	(0.21 -5.06)	
Q3	3.01	(0.73 -12.46)	
Q4	0.72	(0.13 -4.13)	
Thallium			
Q1+Q2	1.00		0.027
Q3+Q4	4.01	(1.18 -13.70)	
Manganese			
Not detected	1.00		0.039
Detected	9.55	(1.12 -81.08)	
Q1	1.00		0.198
Q2	10.22	(0.99 -105.8)	
Q3	11.74	(1.22 -113.3)	
Q4	7.83	(0.82 -74.69)	
Continuous[j]	2.98	(1.04 -8.52)	0.042
Molybdenum			
Not detected	1.00		0.249
Detected	3.56	(0.41 -30.94)	

[continued]

Supplemental Table 4. Continued.

Chemical[a]	OR[b]	(95% CI)	P[c]
Iron			
Q4	1.00		0.567
≤Q3	1.50	(0.37 -6.01)	
Selenium			
≤Q3	1.00		0.713
Q4	1.24	(0.40 -3.85)	
Zinc			
Q1	1.00		0.962
Q2	1.16	(0.27 -5.07)	
Q3	1.39	(0.33 -5.81)	
Q4	1.01	(0.21 -4.83)	
Copper			
Q1	1.00		0.888
Q2	0.59	(0.14 -2.53)	
Q3	0.64	(0.16 -2.66)	
Q4	0.83	(0.19 -3.52)	
Cobalt			
Not detected	1.00		0.382
Detected	1.59	(0.56 -4.49)	
Chromium			
Not detected	1.00		0.136
Detected	3.42	(0.68 -17.26)	
Aluminium			
Not detected	1.00		0.031
Detected	9.62	(1.23 -75.37)	
Tantalum			
Not detected	1.00		0.082
Detected	2.77	(0.88 -8.75)	
Gold			
Not detected	1.00		0.248
Detected	1.85	(0.65 -5.28)	
Bismuth			
Not detected	1.00		0.146
Detected	2.69	(0.71 -10.26)	
Platinum			
Not detected	1.00		0.428
Detected	0.42	(0.05 -3.64)	
Ruthenium[l]			
Not detected	1.00		0.007
Detected	4.22	(1.49 -11.94)	
Sum of orders of lead, thallium, manganese, tantalum, ruthenium, and benzo(b)fluoranthene[i]			
Low	1.00		<0.001
High	9.81	(2.97 -32.38)	

*The odds ratios quantify the magnitude of the associations between the exposures and COVID-19 in the 154 individuals, 20 with COVID-19 and 134 without the disease (see Table 1).
[a] Cut-off points of the concentrations for the exposure categories (quartiles, limits of detection and quantification), and units, are shown in Porta et al., 2023.
[b] Unless otherwise specified, odds ratios were adjusted for PFOS branched (ng/mL, logtransformed), age, smoking, and educational level. [c] Unless otherwise specified, *p*-value derived from Wald's test.
[d] When an individual had DDT and/or DDD detected, and/or DDE in the upper quartile, he was classified as 'high'; when DDT and DDD were not detected and DDE was in any of the 3 lower quartiles, the individual was classified as 'low'. For further details on these sums as well as on the sum of orders, see Porta et al., 2023.
[e] Odds ratio adjusted for PFOS branched (ng/mL, logtransformed), age, and educational level.
[f] Computed by categorizing each PCB in quartiles, and then adding the category number, thus producing a value ranging between 3 and 12.

[g] Arithmetic sum of the concentrations (in ng/g lipid) of PCB congeners 138, 153 and 180.
[h] Multivariate analogue of Mantel's extension test for linear trend.
[i] Odds ratio adjusted for PFOS branched (ng/mL, logtransformed), smoking, and educational level.
[j] Odds ratio for each increase of 10 times in the concentration (lead, µg/dL; manganese, ng/mL).
[k] Odds ratio adjusted for PFOS branched (ng/mL, logtransformed) and age.
[l] Odds ratio adjusted for PFOS branched (ng/mL, logtransformed) and smoking.

Supplemental Table 5. Association of POPs and elements with SARS-CoV-2 seropositivity when adjusting for PFHxS. (N = 145).*

Chemical[a]	OR[b]	(95% CI)	P[c]
***p,p'*-DDT**			
Not detected	1.00		0.188
Detected	3.15	(0.57 -17.33)	
***p,p'*-DDE**			
≤Q3	1.00		0.396
Q4	1.52	(0.58 -3.98)	
***p,p'*-DDD[d]**			
Not detected	1.00		0.119
Detected	7.14	(0.60 -84.62)	
Sum of DDT, DDD and DDE			
Low	1.00		0.439
High	1.46	(0.56 -3.84)	
HCB[d]			
Q1	1.00		0.348
≥Q2	1.56	(0.62 -3.97)	
Sum of orders PCBs 138-153-180[d]			
≤Q3	1.00		0.086
Q4	1.70	(0.62 -4.66)	
PCB 126[d]			
Not detected	1.00		0.346
Detected	2.70	(0.34 -21.24)	
Naphthalene			
Q1	1.00		0.163
≥Q2	2.08	(0.74 -5.84)	
Phenanthrene[d]			
Q1	1.00		0.103
≥Q2	2.11	(0.86 -5.18)	
Fluorene[d]			
Q1	1.00		0.098
≥Q2	2.23	(0.86 -5.78)	
Pyrene			
Q1+Q2	1.00		0.116
Q3+Q4	1.86	(0.86 -4.03)	
Fluoranthene			
Q1	1.00		0.188
≥Q2	1.91	(0.73 -4.99)	
Benzo(b)fluoranthene			
Not detected	1.00		0.102
Detected	5.92	(0.70 -49.99)	
Indene(123,cd)pyrene[d]			
Not detected	1.00		0.608
Detected	2.10	(0.12 -35.36)	
Lead[d]			
Q1	1.00		0.248
Q2	1.56	(0.52 -4.65)	
Q3	1.14	(0.36 -3.67)	
Q4	3.08	(0.90 -10.53)	
≤Q3	1.00		0.060
Q4	2.45	(0.96 -6.20)	
Continuous[e]	4.10	(0.90 -18.72)	0.068

[continued]

Supplemental Table 5. Continued.

Chemical[a]	OR[b]	(95% CI)	P[c]
Silver[d]			
Q1	1.00		0.207
≥Q2	1.85	(0.71 -4.80)	
Thallium[d]			
Q1	1.00		0.016
Q2	1.29	(0.28 -6.07)	
Q3	4.78	(1.59 -14.42)	
Q4	3.91	(1.28 -11.94)	
Q1+Q2	1.00		0.002
Q3+Q4	3.98	(1.69 -9.34)	
Manganese			
Not detected	1.00		0.074
Detected	2.52	(0.92 -6.92)	
Q1	1.00		0.045
Q2	2.06	(0.59 -7.15)	
Q3	4.32	(1.39 -13.45)	
Q4	1.42	(0.40 -5.02)	
Continuous[e]	1.60	(0.85 -2.99)	0.145
Molybdenum			
Not detected	1.00		0.161
Detected	3.05	(0.64 -14.55)	
Iron			
Q4	1.00		0.045
≤Q3	3.09	(1.03 -9.30)	
Selenium			
≤Q3	1.00		0.068
Q4	0.40	(0.15 -1.07)	
Zinc			
Q1	1.00		0.836
Q2	0.60	(0.19 -1.89)	
Q3	0.90	(0.31 -2.60)	
Q4	0.84	(0.28 -2.60)	
Copper			
Q1	1.00		0.606
Q2	0.52	(0.17 -1.57)	
Q3	0.53	(0.18 -1.56)	
Q4	0.76	(0.25 -2.35)	
Chromium			
Not detected	1.00		0.313
Detected	2.05	(0.51 -8.25)	
Aluminium			
Not detected	1.00		0.190
Detected	3.18	(0.56 -17.95)	
Indium			
Not detected	1.00		0.244
Detected	0.58	(0.23 -1.45)	
Tantalum[d]			
Not detected	1.00		0.178
Detected	1.80	(0.77 -4.24)	
Gold[d]			
Not detected	1.00		0.034
Detected	2.27	(1.06 -4.85)	

[continued]

Supplemental Table 5. Continued.

Chemical[a]	OR[b]	(95% CI)	P[c]
Bismuth			
Not detected	1.00		0.230
Detected	1.88	(0.67 -5.28)	
Platinum			
Not detected	1.00		0.248
Detected	0.38	(0.07 -1.98)	
Ruthenium[d]			
Not detected	1.00		0.011
Detected	2.96	(1.28 -6.82)	
Sum of orders of lead, thallium, manganese, tantalum, ruthenium, and benzo(b)fluoranthene[d]			
Low	1.00		<0.001
High	5.37	(2.37 -12.15)	

*The odds ratios quantify the magnitude of the associations between the exposures and SARS-CoV-2 seropositivity in the 145 individuals, 41 SARS-CoV-2 seropositives and 104 seronegatives (see Supplemental Table 5). An OR of 1.00 denotes the reference category.

[a] Cut-off points of the concentrations for the exposure categories (quartiles, limits of detection and quantification) are shown in Porta et al., 2023.

[b] Unless otherwise specified, odds ratios adjusted for PFHxS, household outdoor index, and smoking.

[c] Wald's test.

[d] Odds ratio adjusted for PFHxS and household outdoor index.

[e] Odds ratio for each increase of 10 times in the concentration (lead, µg/dL; manganese, ng/mL).

Supplemental Figure 1. Heatmap of correlations between concentrations of PFAS and persistent organic pollutants (N=240).

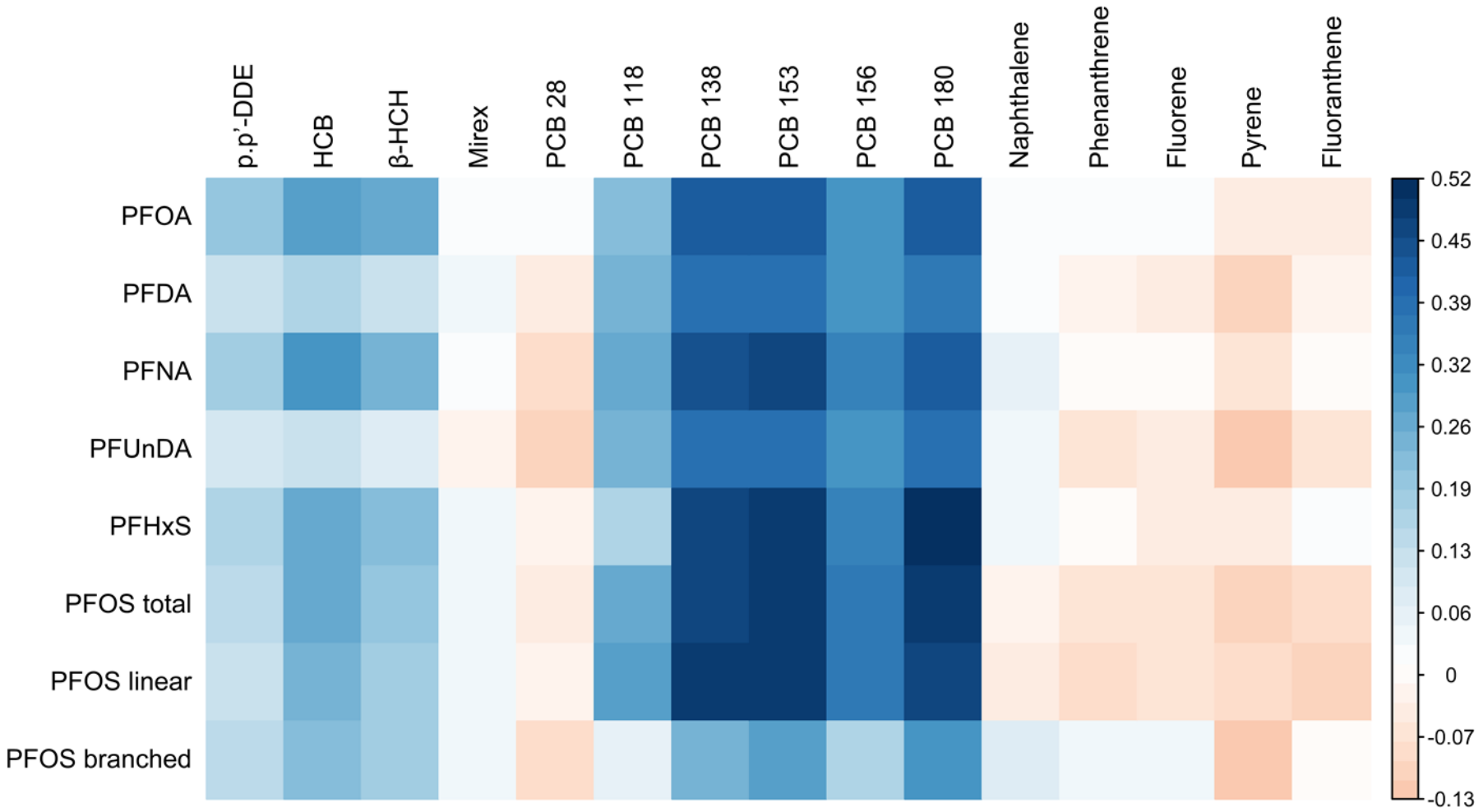

Supplemental Figure 2. Heatmap of correlations between concentrations of PFAS and elements (N=240).